
CHAPTER

1

HISTORICAL OVERVIEW

Superconductivity was discovered in 1911 by H. Kamerlingh Onnes¹ in Leiden, just 3 years after he had first liquefied helium, which gave him the refrigeration technique required to reach temperatures of a few degrees Kelvin. For decades, a fundamental understanding of this phenomenon eluded the many scientists who were working in the field. Then, in the 1950s and 1960s, a remarkably complete and satisfactory theoretical picture of the classic superconductors emerged. This situation was overturned and the subject was revitalized in 1986, when a new class of high-temperature superconductors was discovered by Bednorz and Müller.² These new superconductors seem to obey the same general phenomenology as the classic superconductors, but the basic microscopic mechanism remains an open and contentious question at the time of this writing.

The purpose of this book is to introduce the reader to the field of superconductivity, which remains fascinating after more than 80 years of investigation. To retard early obsolescence, we shall emphasize the aspects which seem to be reasonably securely understood at the present time.

The goal of this introductory chapter is primarily to give some historical perspective to the evolution of the subject. All detailed discussion is deferred to later chapters, where the topics are examined again in much greater depth. We start by reviewing the basic observed electrodynamic phenomena and their early

¹H. Kamerlingh Onnes, *Leiden Comm.* **120b**, **122b**, **124c** (1911).

²G. Bednorz and K. A. Müller, *Z. Phys.* **B64**, 189 (1986).

phenomenological description by the Londons. We then briefly sketch the subsequent evolution of the concepts which are central to our present understanding. This quasi-historical review of the development of the subject is probably too terse to be fully understood on the first reading. Rather, it is intended to provide a quick overview to help orient the reader while reading subsequent chapters, in which the ideas are developed in sufficient detail to be self-contained. In fact, some readers have found this survey more useful to highlight the major points *after* working through the details in subsequent chapters.

1.1 THE BASIC PHENOMENA

What Kamerlingh Onnes observed was that the electrical resistance of various metals such as mercury, lead, and tin disappeared completely in a small temperature range at a critical temperature T_c , which is characteristic of the material. The complete disappearance of resistance is most sensitively demonstrated by experiments with persistent currents in superconducting rings, as shown schematically in Fig. 1.1. Once set up, such currents have been observed to flow without measurable decrease for a year, and a lower bound of some 10^5 years for their characteristic decay time has been established by using nuclear resonance to detect any slight decrease in the field produced by the circulating current. In fact, we shall see that under many circumstances we expect absolutely no change in field or current to occur in times less than 10^{10} years! Thus, *perfect conductivity* is the first traditional hallmark of superconductivity. It is also the prerequisite for most potential applications, such as high-current transmission lines or high-field magnets.

The next hallmark to be discovered was *perfect diamagnetism*, found in 1933 by Meissner and Ochsenfeld.^{3,4} They found that not only a magnetic field is excluded from entering a superconductor (see Fig. 1.2), as might appear to be

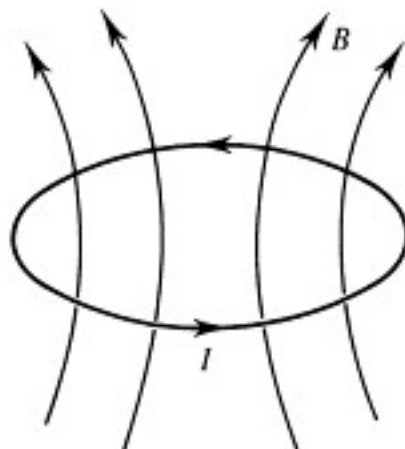
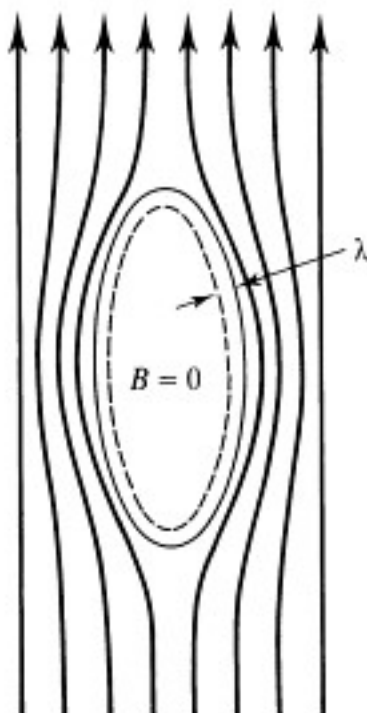


FIGURE 1.1
Schematic diagram of persistent current experiment.

³W. Meissner and R. Ochsenfeld, *Naturwissenschaften* **21**, 787 (1933).

⁴Actually, the diamagnetism is perfect only for *bulk* samples, since the field does penetrate a finite distance λ , typically approximately 500 Å.

**FIGURE 1.2**

Schematic diagram of exclusion of magnetic flux from interior of massive superconductor. λ is the penetration depth, typically only 500 Å.

explained by perfect conductivity, but also that a field in an originally normal sample is *expelled* as it is cooled through T_c . This certainly could *not* be explained by perfect conductivity, which would tend to trap flux *in*. The existence of such a reversible *Meissner effect* implies that superconductivity will be destroyed by a critical magnetic field H_c , which is related thermodynamically to the free-energy difference between the normal and superconducting states in zero field, the so-called condensation energy of the superconducting state. More precisely, this *thermodynamic critical field* H_c is determined by equating the energy $H^2/8\pi$ per unit volume, associated with holding the field out against the magnetic pressure, with the condensation energy. That is,

$$\frac{H_c^2(T)}{8\pi} = f_n(T) - f_s(T) \quad (1.1)$$

where f_n and f_s are the Helmholtz free energies per unit volume in the respective phases in zero field. It was found empirically that $H_c(T)$ is quite well approximated by a parabolic law

$$H_c(T) \approx H_c(0)[1 - (T/T_c)^2] \quad (1.2)$$

illustrated in Fig. 1.3. While the transition in zero field at T_c is of second order, the transition in the presence of a field is of first order since there is a discontinuous change in the thermodynamic state of the system and an associated latent heat.

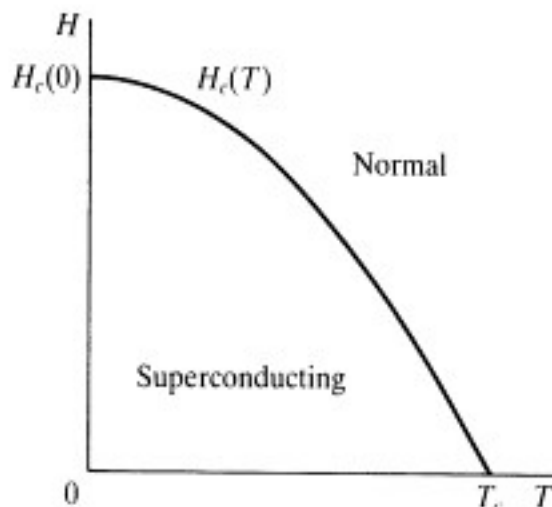


FIGURE 1.3
Temperature dependence of the critical field.

1.2 THE LONDON EQUATIONS

These two basic electrodynamic properties, which give superconductivity its unique interest, were well described in 1935 by the brothers F. and H. London,⁵ who proposed two equations to govern the microscopic electric and magnetic fields

$$\mathbf{E} = \frac{\partial}{\partial t} (\Lambda \mathbf{J}_s) \quad (1.3)$$

$$\mathbf{h} = -c \operatorname{curl} (\Lambda \mathbf{J}_s) \quad (1.4)$$

where

$$\Lambda = \frac{4\pi\lambda^2}{c^2} = \frac{m}{n_s e^2} \quad (1.5)$$

is a phenomenological parameter. It was expected that n_s , the *number density of superconducting electrons*, would vary continuously from zero at T_c to a limiting value of the order of n , the density of conduction electrons, at $T \ll T_c$. In (1.4), we introduce our notational convention of using \mathbf{h} to denote the value of the flux density on a microscopic scale, reserving \mathbf{B} to denote a macroscopic average value. Although notational symmetry would suggest using \mathbf{e} for the microscopic local value of \mathbf{E} in the same way, to avoid constant confusion with the charge e of the electron, we shall do so only in the few cases⁶ where it is really useful. These notational conventions are discussed further in the appendix.

⁵F. and H. London, *Proc. Roy. Soc. (London)* **A149**, 71 (1935).

⁶The fundamental basis for our notational asymmetry in treating \mathbf{E} and \mathbf{B} is in the Maxwell equations $\operatorname{curl} \mathbf{h} = 4\pi\mathbf{J}/c$ and $\operatorname{curl} \mathbf{e} = -(1/c)\partial\mathbf{h}/\partial t$. Superconductors in equilibrium can have nonzero \mathbf{J}_s , as described by the London equations, causing \mathbf{h} to vary on the scale of λ . But in equilibrium, or even steady state, $\partial\mathbf{h}/\partial t = 0$, so that \mathbf{e} is zero, or at least constant in space, so the use of both \mathbf{e} and \mathbf{E} offers no advantage. The distinction is useful only in discussing time-dependent phenomena such as motion of flux-bearing vortices in type II superconductors.

The first of these equations (1.3) describes perfect conductivity since any electric field *accelerates* the superconducting electrons rather than simply sustaining their velocity against resistance as described in Ohm's law in a normal conductor. The second London equation (1.4), when combined with the Maxwell equation $\text{curl } \mathbf{h} = 4\pi\mathbf{J}/c$, leads to

$$\nabla^2 \mathbf{h} = \frac{\mathbf{h}}{\lambda^2} \quad (1.6)$$

This implies that a magnetic field is exponentially screened from the interior of a sample with penetration depth λ , i.e., the Meissner effect. Thus, the parameter λ is operationally defined as a penetration depth; empirically, the temperature dependence of λ is found to be approximately described by

$$\lambda(T) \approx \lambda(0)[1 - (T/T_c)^4]^{-1/2} \quad (1.7)$$

The implications of the London equations are illustrated much more thoroughly in Chap. 2.

A simple, but unsound, "derivation" of (1.3) can be given by computing the response to a uniform electric field of a perfect normal conductor, i.e., a free-electron gas with mean free path $\ell = \infty$. In that case, $d(m\mathbf{v})/dt = e\mathbf{E}$, and since $\mathbf{J} = ne\mathbf{v}$, (1.3) follows. But this computation is not rigorous for the spatially nonuniform fields in the penetration depth, for which (1.3) and (1.4) are most useful. The fault is that the response of an electron gas to electric fields is non-local; i.e., the current at a point is determined by the electric field averaged over a region of radius $\sim \ell$ about that point. Consequently, only fields that are uniform over a region of this size give a full response; in particular, the conductivity becomes *infinite* as $\ell \rightarrow \infty$ only for fields filling all space. Since we are dealing here with an interface between a region with field and one with no field, it is clear that even for $\ell = \infty$, the effective conductivity would remain finite. For the case of a high-frequency current, this corresponds to the extreme anomalous limit of the normal skin effect, in which the surface resistance remains finite even as $\ell \rightarrow \infty$.

A more profound motivation for the London equations is the quantum one, emphasizing use of the vector potential \mathbf{A} , given by F. London⁷ himself. Noting that the canonical momentum \mathbf{p} is $(m\mathbf{v} + e\mathbf{A}/c)$, and arguing that in the absence of an applied field we would expect the ground state to have zero net momentum (as shown in a theorem⁸ of Bloch), we are led to the relation for the local average velocity in the presence of the field

$$\langle \mathbf{v}_s \rangle = \frac{-e\mathbf{A}}{mc}$$

⁷F. London, *Superfluids*, vol. I, Wiley, New York, 1950.

⁸This theorem is apparently unpublished, though famous. See p. 143 of the preceding reference.

This will hold if we postulate that for some reason the wavefunction of the superconducting electrons is “rigid” and retains its ground-state property that $\langle \mathbf{p} \rangle = 0$. Denoting the number density of electrons participating in this rigid ground state by n_s , we then have

$$\mathbf{J}_s = n_s e \langle \mathbf{v}_s \rangle = \frac{-n_s e^2 \mathbf{A}}{mc} = \frac{-\mathbf{A}}{\Lambda c} \quad (1.8)$$

Taking the time derivative of both sides yields (1.3) and taking the curl leads to (1.4). Thus, (1.8) contains both London equations in a compact and suggestive form.⁹

This argument of London leaves open the actual value of n_s , but a natural upper limit is provided by the total density of conduction electrons n . If this is inserted in (1.5), we obtain

$$\lambda_L(0) = \left(\frac{mc^2}{4\pi n e^2} \right)^{1/2} \quad (1.9)$$

The notation here is chosen to indicate that this is an ideal theoretical limit as $T \rightarrow 0$. Note that n_s is expected to decrease continuously to zero as $T \rightarrow T_c$, causing $\lambda(T)$ to diverge at T_c as described by (1.7). Careful comparisons of the rf penetration depths of samples in the normal and superconducting states have shown that the superconducting penetration depths λ are always larger than $\lambda_L(0)$, even after an extrapolation of the data to $T = 0$. The quantitative explanation of this excess penetration depth required introduction of an additional concept by Pippard: the coherence length ξ_0 .

1.3 THE PIPPARD NONLOCAL ELECTRODYNAMICS

Pippard¹⁰ introduced the coherence length while proposing a nonlocal generalization of the London equation (1.8). This was done in analogy to Chambers's nonlocal generalization¹¹ of Ohm's law from $\mathbf{J}(\mathbf{r}) = \sigma \mathbf{E}(\mathbf{r})$ to

$$\mathbf{J}(\mathbf{r}) = \frac{3\sigma}{4\pi\ell} \int \frac{\mathbf{R}[\mathbf{R} \cdot \mathbf{E}(\mathbf{r}')]}{R^4} e^{-R/\ell} d\mathbf{r}'$$

⁹Since (1.8) is evidently not gauge-invariant, it will only be correct for a particular gauge choice. This choice, known as the London gauge, is specified by requiring that $\text{div } \mathbf{A} = 0$ (so that $\text{div } \mathbf{J} = 0$), that the normal component of \mathbf{A} over the surface be related to any supercurrent through the surface by (1.8), and that $\mathbf{A} \rightarrow 0$ in the interior of bulk samples.

¹⁰A. B. Pippard, *Proc. Roy. Soc. (London)* A216, 547 (1953).

¹¹This approach of Chambers is discussed, e.g., in J. M. Ziman, *Principles of the Theory of Solids*, Cambridge University Press, New York (1964), p. 242.

where $\mathbf{R} = \mathbf{r} - \mathbf{r}'$; this formula takes into account the fact that the current at a point \mathbf{r} depends on $\mathbf{E}(\mathbf{r}')$ throughout a volume of radius $\sim \ell$ about \mathbf{r} . Pippard argued that the superconducting wavefunction should have a similar characteristic dimension ξ_0 which could be estimated by an uncertainty-principle argument, as follows: Only electrons within $\sim kT_c$ of the Fermi energy can play a major role in a phenomenon which sets in at T_c , and these electrons have a momentum range $\Delta p \approx kT_c/v_F$, where v_F is the Fermi velocity. Thus,

$$\Delta x \gtrsim \hbar/\Delta p \approx \hbar v_F/kT_c$$

leading to the definition of a characteristic length

$$\xi_0 = a \frac{\hbar v_F}{kT_c} \quad (1.10)$$

where a is a numerical constant of order unity, to be determined. For typical elemental superconductors such as tin and aluminum, $\xi_0 \gg \lambda_L(0)$. If ξ_0 represents the smallest size of a wave packet that the superconducting charge carriers can form, then one would expect a weakened supercurrent response to a vector potential $\mathbf{A}(\mathbf{r})$ which did not maintain its full value over a volume of radius $\sim \xi_0$ about the point of interest. Thus, ξ_0 plays a role analogous to the mean free path ℓ in the nonlocal electrodynamics of normal metals. Of course, if the ordinary mean free path is less than ξ_0 , one might expect a further reduction in the response to an applied field.

Collecting these ideas into a concrete form, Pippard proposed replacement of (1.8) by

$$\mathbf{J}_s(\mathbf{r}) = -\frac{3}{4\pi\xi_0\Lambda c} \int \frac{\mathbf{R}[\mathbf{R} \cdot \mathbf{A}(\mathbf{r}')]}{\mathbf{R}^4} e^{-R/\xi} d\mathbf{r}' \quad (1.11)$$

where again $\mathbf{R} = \mathbf{r} - \mathbf{r}'$ and the coherence length ξ in the presence of scattering was assumed to be related to that of pure material ξ_0 by

$$\frac{1}{\xi} = \frac{1}{\xi_0} + \frac{1}{\ell} \quad (1.12)$$

Using (1.11), Pippard found¹² that he could fit the experimental data on both tin and aluminum by the choice of a single parameter $a = 0.15$ in (1.10). [We shall see in Chap. 3 that the microscopic theory of Bardeen, Cooper, and Schrieffer¹³ (BCS) confirms this form, with the numerical constant $a = 0.18$.] For both metals, λ is considerably larger than $\lambda_L(0)$ because $\mathbf{A}(\mathbf{r})$ decreases sharply over a distance $\lambda \ll \xi_0$, giving a weakened supercurrent response, and hence an increased field penetration. Moreover, the increase of λ with the decreasing mean free path predicted by (1.11) and (1.12) was consistent with data on a series

¹²T. E. Faber and A. B. Pippard, *Proc. Roy. Soc. (London)* **A231**, 336 (1955).

¹³J. Bardeen, L. N. Cooper, and J. R. Schrieffer, *Phys. Rev.* **108**, 1175 (1957).

of tin-indium alloys with a varying mean free path. Thus, Pippard's nonlocal electrodynamic equation (1.11) not only fitted the experimental data, but it also anticipated the form of electrodynamics found several years later from the microscopic theory.

1.4 THE ENERGY GAP AND THE BCS THEORY

The next step in the evolution of our understanding of superconductors was the establishment of the existence of an energy gap Δ , of order kT_c , between the ground state and the quasi-particle excitations of the system. This concept had been suggested earlier by Daunt and Mendelssohn¹⁴ to explain the observed absence of thermoelectric effects, and it had been postulated theoretically by various workers.^{15,16} However, the first quantitative experimental evidence arose from precise measurements of the specific heat of superconductors by Corak et al.¹⁷ These measurements showed that the electronic specific heat well below T_c was dominated by an exponential dependence so that

$$C_{es} \approx \gamma T_c a e^{-bT_c/T} \quad (1.13)$$

where the normal-state electronic specific heat is $C_{en} = \gamma T$, and a and b are numerical constants. Such an exponential dependence, with b found to be ~ 1.5 , implies a minimum excitation energy per particle of $\sim 1.5kT_c$.

At about the same time, measurements of electromagnetic absorption in the region of $\hbar\omega \sim kT_c$ were first carried out. Using millimeter-microwave techniques, Biondi et al.¹⁸ reached this region in aluminum, which has a low $T_c \approx 1.2$ K and hence a small gap, but they were not able to carry the measurements to temperatures much below T_c . Working from the far-infrared side as well as from the microwave side, Glover and Tinkham¹⁹ were able to make a more complete study of thin lead films at temperatures far below $T_c \approx 7.2$ K. These measurements and similar ones on tin films could be interpreted quite convincingly in terms of an energy gap of 3 to 4 times kT_c . This result was consistent with the calorimetric one if excitations always were produced in pairs, as would be expected if they obeyed Fermi statistics. The spectroscopic measurement gives

¹⁴J. G. Daunt and K. Mendelssohn, *Proc. Roy. Soc. (London)* **A185**, 225 (1946).

¹⁵See, e.g., V. L. Ginzburg, *Fortschr. Phys.* **1**, 101 (1953) and references cited therein.

¹⁶J. Bardeen, "Theory of Superconductivity," in S. Flügge (ed.), *Handbuch der Physik*, vol. XV, Springer Verlag, Berlin (1956), pp. 303–310. (This article showed explicitly that an energy gap would account for the Pippard nonlocal electrodynamics.)

¹⁷W. S. Corak, B. B. Goodman, C. B. Satterthwaite, and A. Wexler, *Phys. Rev.* **96**, 1442 (1954); **102**, 656 (1956).

¹⁸M. A. Biondi, M. P. Garfunkel, and A. O. McCoubrey, *Phys. Rev.* **102**, 1427 (1956).

¹⁹R. E. Glover and M. Tinkham, *Phys. Rev.* **104**, 844 (1956); **108**, 243 (1957).

the minimum total energy E_g required to create the pair of excitations; the thermal one measures the energy $E_g/2$ per statistically independent particle.

At this point, Bardeen, Cooper, and Schrieffer²⁰ (BCS) produced their epoch-making pairing theory of superconductivity, which forms the subject of Chap. 3. In the BCS theory, it was shown that even a weak attractive interaction between electrons, such as that caused in second order by the electron-phonon interaction, causes an instability of the ordinary Fermi-sea ground state of the electron gas with respect to the formation of bound pairs of electrons occupying states with equal and opposite momentum and spin. These so-called *Cooper pairs* have a spatial extension of order ξ_0 and, crudely speaking, comprise the superconducting charge carriers anticipated in the phenomenological theories.

One of the key predictions of this theory was that a minimum energy $E_g = 2\Delta(T)$ should be required to break a pair, creating two quasi-particle excitations. This $\Delta(T)$ was predicted to increase from zero at T_c to a limiting value

$$E_g(0) = 2\Delta(0) = 3.528kT_c \quad (1.14)$$

for $T \ll T_c$. Not only did this result agree with the measured gap widths, but the BCS prediction for the shape of the absorption edge above $\hbar\omega_g = E_g$ was also in quantitative agreement with the data of Glover and Tinkham. This agreement provided one of the most decisive early verifications of the microscopic theory.

1.5 THE GINZBURG-LANDAU THEORY

Although a considerable body of work followed the appearance of the BCS theory, serving to substantiate its predictions for various processes such as nuclear relaxation and ultrasonic attenuation in which the energy gap and excitation spectrum play a key role, the most exciting developments of the ensuing decade came in another direction. This direction is epitomized by the Ginzburg-Landau (GL) theory of superconductivity, which concentrates entirely on the superconducting electrons rather than on excitations, and was actually proposed in 1950, 7 years before BCS. Ginzburg and Landau²¹ introduced a complex pseudowavefunction ψ as an order parameter within Landau's general theory of second-order phase transitions. This ψ describes the superconducting electrons, and the local density of superconducting electrons (as defined in the London equations) was given by

$$n_s = |\psi(x)|^2 \quad (1.15)$$

²⁰J. Bardeen, L. N. Cooper, and J. R. Schrieffer, *Phys. Rev.* **108**, 1175 (1957).

²¹V. L. Ginzburg and L. D. Landau, *Zh. Eksperim. i Teor. Fiz.* **20**, 1064 (1950).

Then, using a variational principle and working from an assumed series expansion of the free energy in powers of ψ and $\nabla\psi$ with expansion coefficients α and β , they derived the following differential equation for ψ :

$$\frac{1}{2m^*} \left(\frac{\hbar}{i} \nabla - \frac{e^*}{c} A \right)^2 \psi + \beta |\psi|^2 \psi = -\alpha(T) \psi \quad (1.16)$$

Note that this is analogous to the Schrödinger equation for a free particle, but with a nonlinear term. The corresponding equation for the supercurrent

$$\mathbf{J}_s = \frac{e^* \hbar}{i 2m^*} (\psi^* \nabla \psi - \psi \nabla \psi^*) - \frac{e^{*2}}{m^* c} |\psi|^2 \mathbf{A} \quad (1.17)$$

was also the same as the usual quantum-mechanical current expression for particles of charge e^* and mass m^* . With this formalism they were able to treat two features which were beyond the scope of the London theory, namely: (1) nonlinear effects of fields strong enough to change n_s (or $|\psi|^2$) and (2) the spatial variation of n_s . A major early triumph of the theory was in handling the so-called intermediate state of superconductors (discussed in Chap. 2), in which superconducting and normal domains coexist in the presence of $H \approx H_c$. The interface between two such domains is shown schematically in Fig. 1.4.

When first proposed, the theory appeared rather phenomenological, and its importance was not generally appreciated, especially in the western literature. However, in 1959, Gor'kov²² was able to show that the GL theory was, in fact, a limiting form of the microscopic theory of BCS (suitably generalized to deal with spatially varying situations), valid near T_c , in which ψ is directly proportional to the gap parameter Δ . More physically, ψ can be thought of as the wavefunction of the center-of-mass motion of the Cooper pairs. The GL theory is now universally accepted as a masterstroke of physical intuition which embodies in a simple way

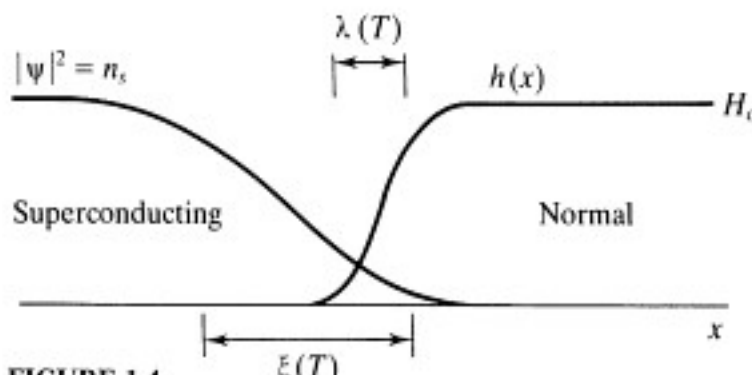


FIGURE 1.4
Interface between superconducting and normal domains in the intermediate state.

²²L. P. Gor'kov, *Zh. Eksperim. i Teor. Fiz.* **36**, 1918 (1959) [Sov. Phys.—JETP **9**, 1364 (1959)].

the macroscopic quantum-mechanical nature of the superconducting state that is crucial for understanding its unique electrodynamic properties.

The GL theory introduces a characteristic length, now usually called the *GL coherence length*,

$$\xi(T) = \frac{\hbar}{|2m^*\alpha(T)|^{1/2}} \quad (1.18)$$

which characterizes the distance over which $\psi(\mathbf{r})$ can vary without undue energy increase. In a pure superconductor far below T_c , $\xi(T) \approx \xi_0$, the (temperature-independent) Pippard coherence length; near T_c , however, $\xi(T)$ diverges as $(T_c - T)^{-1/2}$ since α vanishes as $(T - T_c)$. Thus, these two "coherence lengths" are related but distinct quantities.

The ratio of the two characteristic lengths defines the GL parameter

$$\kappa = \frac{\lambda}{\xi} \quad (1.19)$$

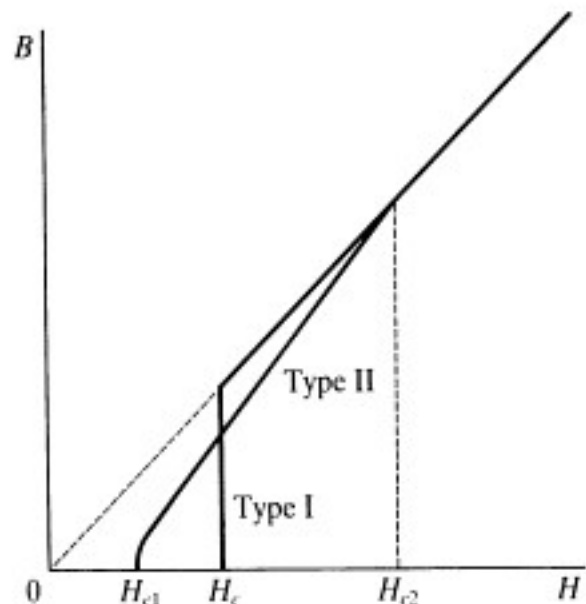
Since λ also diverges as $(T_c - T)^{-1/2}$ near T_c , this dimensionless ratio is approximately independent of temperature. For typical classic pure superconductors, $\lambda \approx 500 \text{ \AA}$ and $\xi \approx 3,000 \text{ \AA}$, so $\kappa \ll 1$. In this case, one can show²³ (see Chap. 4) that there is a positive surface energy associated with a domain wall between normal and superconducting material. This positive surface energy stabilizes a domain pattern in the intermediate state, with a scale of subdivision intermediate between the microscopic length ξ and the macroscopic sample size.

1.6 TYPE II SUPERCONDUCTORS

In 1957 (the same year as BCS), Abrikosov²⁴ published a remarkably significant paper, almost overlooked at the time, in which he investigated what would happen in GL theory if κ were large instead of small, i.e., if $\xi < \lambda$, rather than the reverse. Reversing the argument cited above, this should lead to a *negative* surface energy, so that the process of subdivision into domains would proceed until it is limited by the *microscopic* length ξ , below which the gradient energy term would become excessive. Because this behavior is so radically different from the classic intermediate-state behavior described earlier, Abrikosov called these *type II superconductors* to distinguish them from the earlier *type I* variety. He showed that the exact breakpoint between the two regimes was at $\kappa = 1/\sqrt{2}$. For materials with $\kappa > 1/\sqrt{2}$, he found that instead of discontinuous breakdown of superconductivity in a first-order transition at H_c , there was a continuous increase in flux penetration starting at a lower critical field H_{c1} and reaching $B = H$ at an upper

²³The physical reason is that there is an interfacial layer of thickness $\sim (\xi - \lambda)$ which pays the energetic cost of excluding the magnetic field without enjoying the full condensation energy of the superconducting state.

²⁴A. A. Abrikosov, *Zh. Eksperim. i Teor. Fiz.* **32**, 1442 (1957) [Sov. Phys.—JETP **5**, 1174 (1957)].

**FIGURE 1.5**

Comparison of flux penetration behavior of type I and type II superconductors with the same thermodynamic critical field H_c . $H_{c2} = \sqrt{2}\kappa H_c$. The ratio of B/H_{c2} from this plot also gives the approximate variation of R/R_n , where R is the electrical resistance for the case of negligible pinning, and R_n is the normal-state resistance.

critical field H_{c2} , as shown schematically in Fig. 1.5. Because of the partial flux penetration, the diamagnetic energy cost of holding the field out is less, so H_{c2} (which turns out to be given by $\sqrt{2}\kappa H_c$) can be much greater than the thermodynamic critical field H_c (at which nothing special happens). This property has made possible high-field superconducting magnets.

Another result of Abrikosov's analysis was that, in the so-called *mixed state*, or *Schubnikov phase*, between H_{c1} and H_{c2} , the flux should not penetrate in laminar domains but, rather, in a regular array of flux tubes, each carrying a quantum of flux

$$\Phi_0 = \frac{hc}{2e} = 2.07 \times 10^{-7} \text{ G} - \text{cm}^2 \quad (1.20)$$

Within each unit cell of the array, there is a vortex of supercurrent concentrating the flux toward the vortex center. Although Abrikosov predicted a square array, it was later shown, upon correcting a numerical error, that a triangular array should have a slightly lower free energy. This vortex array was first demonstrated experimentally by a magnetic decoration technique coupled with electron microscopy.²⁵ More recently, scanning tunneling microscope measurements²⁶ have not only

²⁵U. Essmann and H. Träuble, *Phys. Lett.* **24A**, 526 (1967).

²⁶H. F. Hess et al. *Phys. Rev. Lett.* **62**, 214 (1989); *Phys. Rev. Lett.* **64**, 2711 (1990).

confirmed the existence of the vortex array, but they have also made possible detailed measurements of the density of electronic states in the quasi-normal core at the center of each vortex. Of course, random inhomogeneities in the underlying material lead to "pinning" of vortices at favorable locations, so that in some cases one finds a glasslike pattern of flux tubes.

We have already noted that type II superconductors are not perfectly diamagnetic, and since $|\psi|^2$ turns out to go to zero in the centers of the vortices, we are not surprised to find that there is no energy gap in the cores. Thus, we are led to ask whether the first hallmark—perfect conductivity—is also lost. The answer is a bit equivocal, and the details are the subject of ongoing research. In the presence of a transport current, the flux tubes experience a so-called *Lorentz force* $\mathbf{J} \times \Phi_0/c$ per unit length (analogous to the macroscopic force density $\mathbf{J} \times \mathbf{B}/c$) tending to make them move sideways, in which case a longitudinal "resistive" voltage is induced. In an ideal homogeneous material, Bardeen and Stephen²⁷ showed that this flux motion is resisted only by a viscous drag, and that type II superconductors should show a resistance comparable to that in the normal state, only reduced by a factor $\sim B/H_{c2}$. In real materials, however, there is always some inhomogeneity to pin the flux, so that there is essentially no resistance until a finite current is reached, such that the Lorentz force exceeds the pinning force. In superconducting magnet wire, the pinning is deliberately made strong enough to give large critical currents.

1.7 PHASE, JOSEPHSON TUNNELING, AND FLUXOID QUANTIZATION

Faced with these fallen hallmarks, one might well ask what really is the essential universal characteristic of the superconducting state. The answer is the existence of the many-particle condensate wavefunction $\psi(\mathbf{r})$, which has amplitude and phase and which maintains phase coherence over macroscopic distances. This condensate is analogous to, but not identical to, the familiar Bose-Einstein condensate, with Cooper pairs of electrons replacing the single bosons which condense in superfluid helium, for example.

Since the phase and particle number are conjugate variables, reflecting complementary aspects of the wave-particle dualism, there is an uncertainty relation

$$\Delta N \Delta \varphi \gtrsim 1 \quad (1.21)$$

which limits the precision with which N and φ can be simultaneously known. However, since $N \sim 10^{22}$ in a macroscopic sample, both N and φ can be known to within small fractional uncertainties, and the phase may be treated as a semi-classical variable. As we shall see in Chap. 7, however, this is not the case in very small mesoscopic structures.

²⁷J. Bardeen and M. J. Stephen, *Phys. Rev.* **140**, A1197 (1965).

The physical significance of the phase degree of freedom was first emphasized in the work of Josephson,²⁸ who predicted that pairs should be able to tunnel between two superconductors even at zero voltage difference, giving a supercurrent density

$$J = J_c \sin (\varphi_1 - \varphi_2) \quad (1.22)$$

where J_c is a constant and φ_i is the phase of ψ in the i th superconductor at the tunnel junction. He also predicted that a voltage difference V_{12} between the electrodes would cause the phase difference to increase with time as $2eV_{12}t/\hbar$, so that the current would oscillate with frequency $\omega = 2eV_{12}/\hbar$. Although originally received with some skepticism, these predictions have been extremely thoroughly verified. Subsequently, Josephson junctions have been utilized in ultrasensitive voltmeters and magnetometers, and in making the most accurate available measurements of the ratio of fundamental constants h/e . In fact, the standard volt is now *defined* in terms of the frequency of the ac Josephson current.

The most basic implication of the existence of a phase factor in $\psi(\mathbf{r}) \equiv |\psi(\mathbf{r})| e^{i\varphi(\mathbf{r})}$, however, is operative in the simple case of a superconducting ring. In that case, the single-valuedness of ψ requires that $\varphi(\mathbf{r})$ return to itself (modulo 2π) on going once around the ring on any path. Just as the corresponding condition in an atom leads to the quantization of orbital angular momentum in integral multiples of \hbar , here this condition requires that the *fluxoid* Φ' take on only integral multiples of $\Phi_0 = hc/2e$. The fluxoid is a quantity introduced by F. London, which can be written

$$\Phi' = \Phi + \frac{m^* c}{e^*^2} \oint \frac{\mathbf{J}_s \cdot d\mathbf{s}}{|\psi|^2} \quad (1.23)$$

where $\Phi = \oint \mathbf{A} \cdot d\mathbf{s}$ is the ordinary magnetic *flux* through the integration loop. Since the current sustaining the flux in the ring flows only in a layer of thickness $\sim \lambda$ on the inner surface of the ring, if the ring is thick compared to λ , the path of integration can be taken deeper inside the wall of the ring, where $J_s = 0$. Then (1.23) implies that $\Phi = \Phi'$, so that the flux itself has the quantized value $n\Phi_0$. This property was demonstrated experimentally²⁹ in 1961. When J_s is not small, as in the vortices in a type II superconductor, both terms in (1.23) may be equally important, and the value of the flux Φ inside a given contour is itself unrestricted; only the fluxoid Φ' , directly related to the line integral of $d\varphi$, always has precise quantum values.

²⁸B. D. Josephson, *Phys. Lett.* **1**, 251 (1962).

²⁹B. S. Deaver and W. M. Fairbank, *Phys. Rev. Lett.* **7**, 43 (1961); R. Doll and M. Nibauer, *Phys. Rev. Lett.* **7**, 51 (1961).

1.8 FLUCTUATIONS AND NONEQUILIBRIUM EFFECTS

The preceding discussion has been simplified by an implicit assumption that superconductors will always be found in the lowest-energy eigenfunction of the GL equation. While this is indeed the *most probable* single possibility, the presence of the thermal energy $\sim kT$ implies that the system will fluctuate into other low-lying states with a finite probability. At temperatures *below* T_c , the fluctuations which are most prominent are those which allow finite resistance to appear even at currents below the nominal critical current, which is defined as the maximum current before fluctuations of *zero* energy allow a resistive voltage to appear. The other side of the coin is that *above* T_c fluctuations cause some vestiges of superconductivity to remain. These were first observed by Glover,³⁰ who found that the conductivity of amorphous films of superconductors diverges as $(T - T_c)^{-1}$ as one approaches T_c from above. This "Curie-Weiss" form of temperature dependence with an appropriate coefficient was also predicted theoretically at about the same time. Somewhat later, the corresponding effect was also observed³¹ in the diamagnetic susceptibility of pure bulk samples. In this case, the basic divergence is as $(T - T_c)^{-1/2}$.

These measurements and the associated theory show that in principle the effects of the superconducting interaction persist to arbitrarily high temperatures but that in practice a fairly strong cutoff sets in at about $2T_c$. Thus, there is not only some resistance below T_c but also some superconductivity above T_c , although the apparently abrupt switchover observed by Kamerlingh Onnes is still a good working approximation for most purposes. The superconducting transition in the classic superconductors is much sharper than other second-order phase transitions, such as those in magnetic materials, because the coherence length ξ_0 is much larger than the interatomic distance, so that each electron interacts with many others. However, this is not the case in the high-temperature superconductors, where the coherence length is comparable to atomic dimensions, leading to much more prominent fluctuation effects.

In addition to phenomena in which condensate states other than the ground state are explored by thermal fluctuations in the context of thermal equilibrium, *nonequilibrium* regimes have also been studied, as described in Chap. 11. In the simplest examples, energy is fed in from an external source to drive the quasi-particle population out of equilibrium. In this case, one can distinguish two classes of nonequilibrium, involving energy and charge, respectively, as codified by Schmid and Schön.³² The former category includes regimes in which T_c can actually be raised by as much as a factor of 2, but the energy gap Δ is not raised above its equilibrium value at $T = 0$.

³⁰R. E. Glover, III, *Phys. Lett.* **25A**, 542 (1967).

³¹J. P. Gollub, M. R. Beasley, R. S. Newbower, and M. Tinkham, *Phys. Rev. Lett.* **22**, 1288 (1969).

³²A. Schmid and G. Schön, *J. Low Temp. Phys.* **20**, 207 (1975).

1.9 HIGH-TEMPERATURE SUPERCONDUCTIVITY

Finally, we mention the discovery by Bednorz and Müller³³ in 1986 of high-temperature superconductivity in layered materials dominated by copper oxide planes. Materials of this sort have subsequently been discovered with T_c well over 100 K. This has opened the way to a broader range of practical applications than for the classic superconductors because cooling by liquid helium is not required. Realization of these applications has not been immediate, however, because these oxide materials are hard to fabricate in useful forms and have low electron densities compared to conventional metals. Resistance-causing fluctuations are much more prominent than in the classic superconductors for several reasons: (1) Operation at higher temperatures inevitably makes thermal fluctuations more important; (2) using (1.10), the high T_c and the low Fermi velocity stemming from the low electron density implies a short coherence length, which allows easier fluctuations; and (3) the anisotropy induced by the weak interplanar coupling reduces the integrity of vortex lines, so that pinning is less effective. Despite these practical obstacles, the intellectual challenge of understanding these unusual materials has motivated an enormous volume of research, and remarkable progress has been made.

At the time of this writing, the basic physical mechanism responsible for the high T_c is not yet clear. It is clear that a two-electron pairing is involved, but the nature of the pairing (*s* wave vs. *d* wave) remains controversial, although very recent experiments seem to favor *d* wave pairing. Nonetheless, the magnetic properties, including the melting of the flux-line lattice giving easily measurable resistance over a substantial range of fields below $H_{c2}(T)$, can be addressed quite satisfactorily within the framework of a model of a layered superconductor with Josephson coupling between the layers. Such a model was introduced by Lawrence and Doniach³⁴ more than 20 years ago to describe layered low-temperature superconductors. Accordingly, our treatment of high-temperature superconductivity in Chap. 9 will focus primarily on the many implications of the Lawrence-Doniach model for these materials. We shall also include a brief introduction to the Larkin-Ovchinnikov³⁵ theory of collective pinning and flux creep, and to other topics that are not specifically tied to high-temperature superconductivity but which have been illuminated by the intensive theoretical activity on all aspects of superconductivity brought on by its discovery. Finally, we shall briefly review the experimental evidence in favor of unconventional pairing in these materials.

With this quick overview behind us, we now proceed to a more detailed discussion of the topics mentioned in this outline.

³³G. Bednorz and K. A. Müller, *Z. Phys.* **B64**, 189 (1986).

³⁴W. E. Lawrence and S. Doniach, in E. Kanda (ed.), *Proc. 12th Int. Conf. Low Temp. Phys.*, Kyoto, Japan (1970) [Keigaku, Tokyo, (1971)], p. 361.

³⁵A. I. Larkin and Yu. V. Ovchinnikov, *J. Low Temp. Phys.* **34**, 409 (1979).

CHAPTER

2

INTRODUCTION TO ELECTRODYNAMICS OF SUPERCONDUCTORS

In this chapter, we shall work through a number of illustrative examples to get a feeling for the electrodynamic behavior of the classic type I superconductors at the level of the London equations, simply taking the penetration depth $\lambda(T)$ and the critical field $H_c(T)$ as given parameters. This treatment, which avoids the details of the Ginzburg-Landau (GL) theory and the underlying BCS theory, is a good approximation for the cases treated because the GL theory reduces to the London theory when n_s can be taken to have its equilibrium value everywhere, and because the BCS theory introduces qualitative new features *only* at frequencies above the energy gap. In fact, this simple treatment is all that is needed for many applications.

We start by reviewing the physics described by the London equations (1.3) and (1.4) in terms of a simple model. We then illustrate their implications by treating the simple example of a superconducting slab in a parallel dc magnetic field and the effect of the self-field of a current in a wire. Next, we treat the coexistence of superconductivity and normal metal in the so-called *intermediate state* of a type I superconductor in a magnetic field that is comparable to H_c . Finally, we introduce the complex ac conductivity of superconductors and use it to discuss the absorption of electromagnetic radiation at frequencies below the energy gap frequency.

2.1 THE LONDON EQUATIONS

When we introduced the London equations in Sec. 1.2, we pointed out that a classical “derivation” in terms of electrons with infinite mean free path could not be justified in any rigorous way. Nonetheless, such an approach gives a useful physical feeling for the phenomena they describe, and we shall use it here to motivate the form of the equations and also to estimate the value of the penetration depth λ .

In the standard Drude model for electrical conductivity, one applies classical mechanics to the electron motion and writes

$$m \frac{dv}{dt} = eE - mv/\tau$$

Here v is the average or “drift” velocity of the electrons, and τ is a phenomenological relaxation time describing the time it would take the scattering from defects to bring the drift velocity of the electrons to zero. In a normal metal, the competition described by this equation between the scattering and the acceleration by E leads to a steady-state drift velocity $v = eE\tau/m$. If there are n conduction electrons per unit volume, this produces an electric current density $J = nev = (ne^2\tau/m)E = \sigma E$, i.e., Ohm’s law.

Insofar as it is possible to describe the perfect conductivity of a superconductor by postulating that a certain density n_s of its electrons act as if there were no scattering term (by letting their τ_s go to infinity), Ohm’s law is replaced by an *accelerative supercurrent*. That is, we have $dv_s/dt = eE/m$, so that the total supercurrent J_s is governed by

$$dJ_s/dt = (n_s e^2/m)E = E/\Lambda = (c^2/4\pi\lambda^2)E \quad (1.3')$$

which is equivalent to the first London equation (1.3) together with the definition (1.5) of the parameters Λ and λ . (Our notational convention is to use λ to denote the phenomenological penetration depth involving the phenomenological parameter n_s , reserving λ_L to denote the specific theoretical limiting value for a pure superconductor with local electrodynamics, as defined in the BCS theory.)

Taking the time derivative of the Maxwell equation $\nabla \times \mathbf{h} = 4\pi\mathbf{J}/c$, inserting (1.3'), and then eliminating $\partial\mathbf{h}/\partial t$ using the other Maxwell equation $\nabla \times \mathbf{E} = -(1/c) \partial\mathbf{h}/\partial t$, we obtain

$$-\nabla \times \nabla \times \mathbf{E} = \nabla^2 \mathbf{E} = \mathbf{E}/\lambda^2 \quad (2.1a)$$

after using a vector identity. These results apply only to time-varying electric fields since (1.3') would imply a current accelerating to infinity in response to a strictly dc electric field. Equation (2.1a) shows that such a time-dependent electric field is screened out exponentially in a distance λ . By further use of the Maxwell equations, we can show that this result implies that *time-varying magnetic* fields are also screened in this same distance λ .

The essential content of the second London equation (1.4) (which *cannot* be “derived” by a classical argument of this sort) is that this screening of magnetic fields also applies to *time-independent* magnetic fields, as is required to describe

the Meissner effect. This can be seen in detail by taking the curl of both sides of the Maxwell equation $\nabla \times \mathbf{h} = (4\pi/c)\mathbf{J}$ and by substituting $-\mathbf{h}/c\Lambda$ from (1.4) for $\nabla \times \mathbf{J}$. (Recall that our notational convention is that \mathbf{h} represents the microscopic value of the magnetic flux density, whereas \mathbf{B} denotes its macroscopic average.) After noting that $\nabla \cdot \mathbf{h} = 0$ by Maxwell's equations, we see that

$$\nabla^2 \mathbf{h} = (1/\lambda^2)\mathbf{h} \quad (2.1b)$$

with

$$\lambda^2 = mc^2/4\pi n_s e^2 \quad (2.2)$$

as stated in (1.5). Equations (2.1b) and (2.2) can be considered the operational definition of the phenomenological superconducting electron density n_s in terms of the measurable quantity λ .

2.2 SCREENING OF A STATIC MAGNETIC FIELD

The most important consequence of the London equations (1.3) and (1.4), or the derived equations (2.1a,b), is that electromagnetic fields are screened from the interior of a bulk superconductor in a characteristic penetration depth λ , given by (2.2). For example, a particular solution of (2.1b) describes a magnetic field h , parallel to the surface, which decreases exponentially into the interior of a bulk superconductor as

$$h(x) = h(0)e^{-x/\lambda},$$

where x is measured in from the surface. Equation (2.1a) shows that a time-varying *electric* field is screened in the same way.

If one inserts the effective density of conduction electrons n (as determined, e.g., from surface impedance measurements of the electromagnetic skin depth in the normal state) for n_s in (2.2), the predicted value of λ is found to be ~ 200 Å in typical classic metallic conductors. The experimental values of λ for pure samples are typically 500 Å for $T \ll T_c$. As noted in Sec. 1.3, this quantitative discrepancy results from the nonlocal electrodynamics in pure superconductors, which will be discussed further in connection with the BCS theory in Chap. 3. In superconductors with short electronic mean free path ("dirty superconductors") or short coherence length (such as the high-temperature superconductors), the electrodynamics becomes local, as in the London theory. These materials have larger values of λ (typically up to 1500 Å) corresponding to a much smaller value of the phenomenological parameter n_s .

In all these cases, as one approaches the second-order phase transition at T_c , $n_s \rightarrow 0$ continuously; as a result, $\lambda(T)$ diverges as $T \rightarrow T_c$. The BCS theory will account for this temperature dependence, which depends in detail on the ratios of the characteristic lengths λ , ξ , and ℓ but is qualitatively the same in all cases. A frequently used empirical temperature dependence is

$$\lambda(T) \approx \lambda(0)/(1 - t^4)^{1/2} \quad (2.3)$$

In terms of (2.2), this corresponds to n_s going to zero at T_c as $(1 - t^4)$, where $t = T/T_c$ is referred to as the *reduced temperature*. This dependence is often called the *two-fluid temperature dependence*, referring to an early model of Gorter and Casimir,¹ which interpreted the thermodynamics of superconductors in terms of coexisting fluids of normal and “condensed” or superconducting electrons. This model related the measured T dependences of the specific heat and the critical field, and gave this dependence for the density of condensed electrons.

2.2.1 Flat Slab in Parallel Magnetic Field

A classic and important example of the application of the London equations is the case of a flat superconducting slab of finite thickness d in an applied parallel magnetic field H_a . Solving (2.1b) with the boundary conditions that $h = H_a$ at the two surfaces at $x = \pm d/2$, one obtains a superposition of exponentials penetrating from both sides, so that

$$h = H_a \frac{\cosh(x/\lambda)}{\cosh(d/2\lambda)} \quad (2.4)$$

This shows that h is reduced to a minimum value $H_a/\cosh(d/2\lambda)$ at the midplane of the slab. Averaged over the sample thickness d , one finds

$$B \equiv \bar{h} \equiv H_a + 4\pi M = H_a \frac{2\lambda}{d} \tanh \frac{d}{2\lambda} \quad (2.5)$$

It is clear from (2.5) that when $d \gg \lambda$, $B \rightarrow 0$ and $M \rightarrow -H_a/4\pi$. This is the *Meissner effect* limit of perfect diamagnetism of bulk superconductors. On the other hand, when $d \ll \lambda$, series expansion of $\tanh x \approx x - x^3/3 + \dots$ shows that $B \rightarrow H_a(1 - d^2/12\lambda^2)$, so that

$$M \rightarrow -(H_a/4\pi)(d^2/12\lambda^2) \quad (2.5a)$$

Some of the earliest experimental determinations of λ were made by comparing magnetization measurements on thin films with the results of calculations of this sort.

We focus particularly on the magnetization M because of its key role in determining the observed critical field. The reason is that the superconducting state becomes energetically unfavorable above the magnetic field H_m at which the added magnetic energy associated with the diamagnetic response in the superconducting state becomes greater than its initial advantage in free energy in zero field. That is, H_m is determined by the relation

$$(F_n - F_s) |_{H=0} = - \int_0^{H_m} M(H) dH \quad (2.6)$$

¹C. J. Gorter and H. B. G. Casimir, *Phys. Z.* **35**, 963 (1934); *Physica* **1**, 306 (1934).

For the Meissner case, where $M = -H/4\pi$, this maximum field H_m is called the *thermodynamic critical field* for this reason, and is given the special symbol H_c . From (2.6) it is clear that

$$H_c^2/8\pi \equiv (F_n - F_s)|_{H=0} \quad (2.6a)$$

as anticipated in (1.1).

For the case of a thin film that is parallel to the applied field, we insert (2.5a) into (2.6), and see that the critical field is increased from H_c to

$$H_{c\parallel} = \sqrt{12}H_c\lambda/d \quad (2.6b)$$

[Although this result is qualitatively correct, the full GL theory (see Chap. 4) replaces the factor $\sqrt{12}$ by $\sqrt{24}$.] To give a numerical example, a 100 Å thick film of tin, which has $\lambda \approx 500$ Å and $H_c \approx 300$ Oe, will have $H_{c\parallel} \approx 7,500$ Oe $\gg H_c$. This great increase in the critical magnetic field of a thin film in a parallel magnetic field is an important thermodynamic consequence of the fact that its magnetization M is greatly reduced below the Meissner value.

2.2.2 Critical Current of Wire

Consider a long superconducting wire of circular cross section with radius $a \gg \lambda$, carrying a current I . This current produces a circumferential self-field at the surface of the wire of magnitude $H = 2I/ca$. When this field reaches the critical field H_c , it will destroy the superconductivity. (This is the so-called *Silsbee criterion*.) Thus, the critical current will be $I_c = caH_c/2$, which scales with the *perimeter*, not the cross-sectional area, of the wire. This suggests that the current flows only in a surface layer of constant thickness. It can be confirmed analytically by application of the London and Maxwell equations in this geometry that this is so, and that the thickness of the surface layer is λ . Since the cross-sectional area of this surface layer will be $2\pi a\lambda$, the critical current density J_c will be $I_c/2\pi a\lambda$, namely,

$$J_c = \frac{c}{4\pi} \frac{H_c}{\lambda} \quad (2.7)$$

Although this argument in terms of the critical field cannot be used to show it, more general energetic arguments indicate that this value of J_c also holds for wires that are much thinner than λ , where the current density is nearly uniform and I_c is proportional to the cross-sectional area. [Again, the full GL theory (see Chap. 4) gives a result differing by a numerical factor of $(2/3)^{3/2} \sim 0.5$.] Putting typical numerical values $H_c = 500$ Oe and $\lambda = 500$ Å in (2.7), one finds that J_c is typically of order 10^8 A/cm², a very large value indeed.

2.3 TYPE I SUPERCONDUCTORS IN STRONG MAGNETIC FIELDS: THE INTERMEDIATE STATE

We now consider the effect of fields strong enough to destroy superconductivity, rather than simply induce screening currents to keep the field out of the interior of the sample. The effect of such fields depends on the *shape* of the sample. The simplest case is that of a long, thin cylinder or sheet, parallel to the field, such as the slab treated in the previous section, because in this case the field everywhere along the surface is just equal to the applied field H_a . For other geometries, in which the demagnetizing factor of the sample is *not* zero, the field over part of the surface will exceed the applied field, as is illustrated in Fig. 2.1, causing some normal regions to appear while H_a is still less than H_c .

Let us now consider the relevant free energies in some detail, restricting our attention at first to the simple case of zero demagnetizing factor. When the sample (of volume V) is normal, the total Helmholtz free energy is given by

$$F_n = Vf_{n0} + V\frac{H_a^2}{8\pi} + V_{\text{ext}}\frac{H_a^2}{8\pi} \quad (2.8)$$

where f_{n0} is the free-energy density in the normal state in the absence of the field, and the terms in H_a^2 denote the energy of the field inside and outside the sample, respectively. When the sample is superconducting, the Meissner effect excludes the field from the interior, so that

$$F_s = Vf_{s0} + V_{\text{ext}}\frac{H_a^2}{8\pi} \quad (2.9)$$

where f_{s0} is the free-energy density in the superconducting state. (We assume macroscopic sample dimensions, so that it is permissible to ignore the effects of field penetration and currents in a layer λ deep on the surface.) Taking the difference, we have

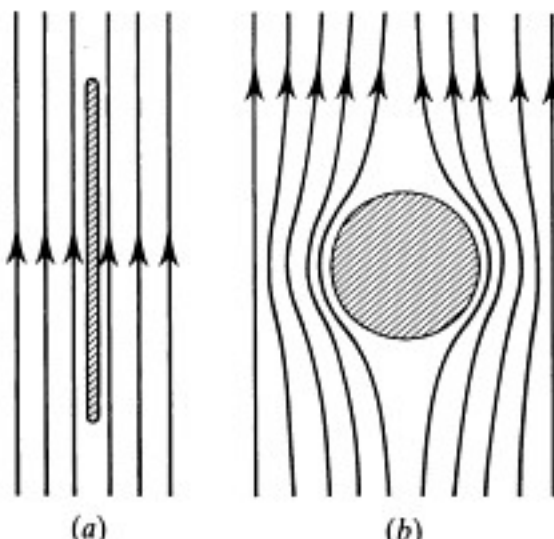


FIGURE 2.1
Contrast of exterior-field pattern (a) when demagnetizing coefficient is nearly zero and (b) when it is $\frac{1}{3}$ for a sphere. In (b) the equatorial field is three halves the applied field for the case of full Meissner effect, which is shown.

$$\begin{aligned} F_n - F_s &= V(f_{n0} - f_{s0}) + \frac{VH_a^2}{8\pi} \\ &= V\left(\frac{H_c^2}{8\pi}\right) + V\left(\frac{H_a^2}{8\pi}\right) \end{aligned} \quad (2.10)$$

In the second form, we have used the defining relation for the thermodynamic critical field H_c

$$f_{n0} - f_{s0} = \frac{H_c^2}{8\pi} \quad (2.11)$$

In particular, when $H_a = H_c$, (2.10) becomes

$$F_n - F_s|_{H_c} = V\left(\frac{H_c^2}{4\pi}\right) \quad (2.12)$$

Thus, at the transition from the superconducting to the normal state, the free energy F increases by $H_c^2/4\pi$ per unit volume. Where does the energy come from? It comes from the energy source maintaining the constant field doing work against the back emf (electromotive force) induced as the flux enters the sample, as can be shown by an elementary computation.

The reason for the awkward necessity of considering the energy of the source of the field is that we carried out the preceding discussion in terms of the Helmholtz free energy. This free energy is appropriate for situations in which \mathbf{B} is held constant rather than \mathbf{H} because if \mathbf{B} is constant, there is no induced emf and no energy input from the current generator. The appropriate thermodynamic potential for the case of constant \mathbf{H} is the Gibbs free energy G . This differs from F by the term $-V(BH/4\pi)$, which essentially accounts automatically for the work² done by the generator. Thus, we consider the Gibbs free-energy density

$$g = f - \frac{hH}{4\pi} \quad (2.13)$$

This leads to

$$G_n = Vf_{n0} - \frac{VH_a^2}{8\pi} - \frac{V_{\text{ext}}H_a^2}{8\pi} \quad (2.14)$$

since $\mathbf{h} = \mathbf{B} = \mathbf{H}$ in the normal state and outside the sample, whereas

$$G_s = Vf_{s0} - \frac{V_{\text{ext}}H_a^2}{8\pi} \quad (2.15)$$

²For a discussion of magnetic work, see, e.g., F. Reif, *Fundamentals of Statistical and Thermal Physics*, McGraw-Hill, New York (1965), pp. 439–444.

since $\mathbf{h} = \mathbf{B} = 0$ in the superconducting state. Taking the difference yields

$$G_n - G_s = V(f_{n0} - f_{s0}) - \frac{VH_a^2}{8\pi} \quad (2.16)$$

Because the requirement for phase equilibrium is the equality of the normal and superconducting values of the appropriate thermodynamic potential, which is G for the case of fixed \mathbf{H} , (2.16) together with the definition of H_c given in (2.11) imply that $H_a = H_c$ is the condition for coexistence of superconducting and normal phases in equilibrium.

2.3.1 Nonzero Demagnetizing Factor

The preceding discussion was, of course, an idealization for the sake of simplicity. Any real sample will have a nonzero demagnetizing factor, which will cause the field at the surface to be different from H_a , the uniform applied field at large distances from the sample. As a concrete example, let us treat the case of a spherical superconducting sample of radius R . On a macroscopic scale, we still have $\mathbf{B} = 0$ inside the superconductor, at least for $H_a \ll H_c$. Outside, the field satisfies

$$\nabla \cdot \mathbf{B} = \nabla \times \mathbf{B} = \nabla^2 \mathbf{B} = 0 \quad (2.17a)$$

with boundary conditions

$$\mathbf{B} \rightarrow \mathbf{H}_a \text{ as } r \rightarrow \infty \quad (2.17b)$$

$$B_n = 0 \text{ at } r = R \quad (2.17c)$$

where B_n is the normal component of \mathbf{B} . This is a standard boundary-value problem, with exterior solution

$$\mathbf{B} = \mathbf{H}_a + \frac{H_a R^3}{2} \nabla \left(\frac{\cos \theta}{r^2} \right) \quad (2.18)$$

where θ is the polar angle measured from the direction of \mathbf{H}_a . It can readily be verified that (2.18) satisfies all the conditions of (2.17), including $B_n = 0$. Similarly, a direct calculation shows that the surface tangential component of \mathbf{B} is

$$(B_\theta)_R = \frac{3}{2} H_a \sin \theta \quad (2.19)$$

Note that this exceeds H_a over an equatorial band of angles from $\theta = 42^\circ$ to 138° . At the equator, $B_\theta = 3H_a/2$, so that the equatorial field reaches H_c as soon as H_a reaches $2H_c/3$. Therefore, for even slightly higher H_a , certain regions of the sphere must go normal. Still, the whole sphere cannot go normal since if it did, the diamagnetism would disappear completely, leaving $H = H_a \approx 2H_c/3$ everywhere, a value insufficient to keep the superconductivity from reappearing. Thus, for fields in the range

$$\frac{2H_c}{3} < H_a < H_c$$

there must be a coexistence of superconducting and normal regions, which, following historical usage, is called *the intermediate state*. The size of the superconducting and normal regions depends on the value of the (positive) interfacial energy. If this energy were zero (or negative), the subdivision could be finer than λ and the Meissner effect would not be observed.³

Generalizing to other ellipsoidal shapes (for which alone a demagnetizing factor is well defined), we expect an intermediate state whenever the applied field lies in range

$$1 - \eta < \frac{H_a}{H_c} < 1 \quad (2.20)$$

The demagnetizing factor η as defined here ranges from zero for the limit of a long, thin cylinder or thin plate in a parallel field to $\frac{1}{3}$ for a sphere to $\frac{1}{2}$ for a cylinder in a transverse field and finally to unity for an infinite flat slab in a perpendicular field. Because the slab in a perpendicular field *always* shows the intermediate state, we treat that limiting case in the greatest detail. It is also the configuration in which most experimental studies of the intermediate state have been carried out.

2.3.2 Intermediate State in a Flat Slab

Let us consider an infinite flat slab of thickness $d \gg \lambda$ in a perpendicular field, a problem first treated in a classic paper of Landau.⁴ In this case, it is appropriate to consider the average flux per unit area in the slab to be fixed by the source at a value B_a , which will equal the external field far enough from the slab that any inhomogeneities induced by the slab will average out. (See Fig. 2.2) Since $h = 0$ in the superconducting regions, the fraction ρ_n of normal material must then be related to the flux density h_n in it by

$$\rho_n = \frac{B_a}{h_n} \quad (2.21)$$

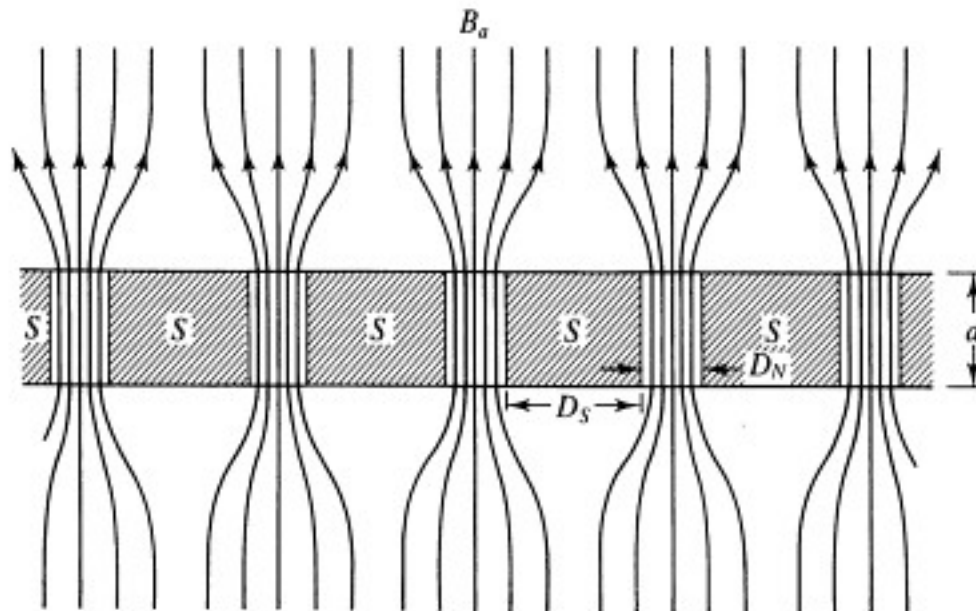
Neglecting surface-energy effects, $h_n = H_c$, as expected from (2.16), but there will be corrections to this value.

To find the scale and shape of the superconducting and normal regions, we need to consider surface energies in the energy balance. We group these into two terms: F_1 , arising from the interfaces within the slab between superconducting (S) and normal (N) domains, and F_2 , dominantly dependent on the behavior near the interface between the sample and the space outside.

Since our discussion so far is limited to situations in which the superconductivity is constant in space, we must anticipate our later development of the Ginzburg-Landau (GL) theory (which can deal with spatial gradients) by

³F. London, *Superfluids*, vol. I, Wiley, New York (1950), p. 128.

⁴L. D. Landau, *Phys. Z. Sowjet.*, **11**, 129 (1937).

**FIGURE 2.2**

Schematic diagram showing magnetic flux channeling through the normal laminae in the intermediate state of a type I superconductor. Flux density is B_a at large distances and zero or $h_n (\approx H_c)$ in the cross section of the slab. The normal regions are macroscopic, in contrast to the vortices in a type II superconductor, which contain only a single quantum of flux.

introducing a phenomenological surface-energy term associated with the NS interface. This is usually expressed in terms of a length, which we shall denote⁵ $\delta(T)$, such that the additional energy per unit area of interface is

$$\gamma = \frac{H_c^2}{8\pi} \delta \quad (2.22)$$

Since it will turn out that $\delta \approx \xi - \lambda$, δ is positive and of order 10^{-5} to 10^{-4} cm for typical type I superconductors. If the surface energy were negative, we could not have a stable equilibrium of macroscopic volumes of the two phases. Instead, the interfaces would proliferate to gain negative surface energy. This is essentially what we shall find happens in type II superconductors. For the present, then, we take γ to be positive.

Given a positive interface energy γ , the domain walls will assume a configuration of minimum area, all other considerations being equal. In particular, given a pattern of normal regions at the surface (which determines the energy F_2 mentioned earlier), the domain walls will to a good approximation run straight through the slab perpendicular to the surface, since any other choice would increase F_1 . It is less clear what the two-dimensional domain pattern should be since it involves optimizing the trade-off between interface energy within the sample (F_1) and field energy just outside the sample (F_2). No rigorous solutions have been found in any

⁵Another common notation is $\Delta(T)$; we avoid this to prevent confusion with the energy gap.

generality; rather, various models are compared. From such studies⁶ it has become clear that the free-energy differences are small between even radically different geometries (such as laminae and tubes of normal material), so long as the scale of the structure is optimized in each case. This suggests that many different configurations will be found, depending on the exact experimental conditions and the sample quality, and this expectation is borne out in practice.⁷

Because of its analytical simplicity, and because it is representative of actual observed structures, we shall concentrate on an analysis of the laminar model of the intermediate state. In this model, there is a one-dimensional array of alternating *N* and *S* domains, of thickness D_n and D_s , with period $D = D_n + D_s$, as illustrated in Fig. 2.2. The interface energy F_1 per unit area of the slab is then readily seen to be

$$F_1 = \frac{2d\gamma}{D} = \frac{2}{D} \frac{d\delta H_c^2}{8\pi} \quad (2.23)$$

By itself, this term favors a very coarse structure, but the exterior term F_2 works in the opposite direction, as we now show.

Although numerical calculations of F_2 were carried out by Landau and his coworkers, we shall content ourselves with a simple physical argument which gives quite similar results. The dominant contribution to F_2 is the energy of the nonuniform external magnetic field outside the domain structure of the intermediate state relative to that of the uniform field which is there if the sample is in the normal state or has an infinitely finely divided domain pattern. At the surface, the average energy density of the field is

$$\frac{\rho_n h_n^2}{8\pi}$$

since a fraction ρ_n of the volume has a field h_n , whereas, using (2.21), the energy density of the uniform field is

$$\frac{B_a^2}{8\pi} = \frac{\rho_n^2 h_n^2}{8\pi}$$

Thus, the average excess energy density at the surface due to the domain structure is

$$\frac{(\rho_n - \rho_n^2)h_n^2}{8\pi} = \frac{\rho_n \rho_s h_n^2}{8\pi} \quad (2.24)$$

⁶See, e.g., E. R. Andrew, *Proc. Roy. Soc. (London)* **A194**, 98 (1948); R. N. Goren and M. Tinkham, *J. Low Temp. Phys.*, **5**, 465 (1971).

⁷For photographs, see, e.g., R. P. Huebener, *Magnetic Flux Structures in Superconductors*, Springer (1979), Chap. 2; J. D. Livingston and W. DeSorbo, "The Intermediate State in Type I Superconductors," in R. D. Parks (ed.), *Superconductivity*, Dekker, New York (1969), p. 1235; A. C. Rose Innes and E. H. Rhoderick, *Introduction to Superconductivity*, 2nd ed., Pergamon, Oxford (1978); T. E. Faber, *Proc. Roy. Soc. (London)* **A248**, 460 (1958).

where $\rho_s = 1 - \rho_n$ is the superconducting fraction. Above the surface, the field inhomogeneity leading to this excess energy will be substantially reduced in a "healing length" L , which will be of the order of the lesser of the lengths D_n and D_s . A convenient mathematical form embodying this observation is

$$L = (D_n^{-1} + D_s^{-1})^{-1} = \frac{D}{\rho_n^{-1} + \rho_s^{-1}} = D\rho_s \rho_n$$

Approximating F_2 by the excess energy density (2.24) out to a distance L on either side of the slab, we have

$$F_2 = \frac{2\rho_n^2 \rho_s^2 D h_n^2}{8\pi} . \quad (2.25)$$

If we now minimize the sum of F_1 and F_2 with respect to D , we find

$$D = \frac{(d\delta)^{1/2} H_c}{\rho_n \rho_s h_n} \approx \frac{(d\delta)^{1/2}}{\rho_n \rho_s} \quad (2.26)$$

as the period of the domain structure. Note that its order of magnitude is set by the geometric mean of a macroscopic dimension, the sample thickness d , and a microscopic dimension, the domain-wall thickness δ . For typical values, $D \approx 10^{-2}$ cm. Another characteristic feature is that the number of domains becomes small (i.e., D becomes large) when either ρ_n or ρ_s is small, i.e., near $B_a = 0$ or H_c .

Such domain patterns have been observed experimentally⁸ by such varied techniques as: (1) moving a tiny magnetoresistive or Hall-effect probe over the surface, (2) making powder patterns with either ferromagnetic or superconducting (diamagnetic) powders which outline the flux-bearing regions, and (3) using the Faraday magneto-optic effect in magnetic glasses in contact with the surface. Orderly laminar patterns are favored if the magnetic field is applied at an angle to the normal, causing laminae aligned with the field direction to have less domain-wall area and hence lower energy. From measurements on such structures, values of the surface-energy parameter δ have been obtained which are in satisfactory agreement with theoretical expectations based on the GL theory. In fact, these measurements played an important role in establishing that theory in the first place.

In addition to determining the scale of the domain structure, the surface energy also depresses the critical field in the intermediate state to a value H_{cl} , which is somewhat below H_c , the critical field for the case of zero demagnetizing factor. (Do not confuse this H_{cl} for a type I superconductor in the intermediate state with the H_{c1} of a type II superconductor.) We may estimate the size of this effect by computing the surface energy $F_1 + F_2$ with the optimized domain size D

⁸Access to this extensive literature is provided by the review of J. D. Livingston and W. DeSorbo, in R. D. Parks (ed.), *Superconductivity*, Dekker, New York (1969), Chap. 21.

given by (2.26) and by adding it to the volume energy terms, appropriately weighted with ρ_n or ρ_s . The resulting average free energy per unit volume of sample is

$$\begin{aligned} f_I &= \rho_s f_{s0} + \rho_n \left(f_{s0} + \frac{H_c^2}{8\pi} + \frac{h_n^2}{8\pi} \right) + \frac{F_1 + F_2}{d} \\ &= f_{s0} + \rho_n \frac{H_c^2}{8\pi} + \frac{B_a^2}{\rho_n 8\pi} + 4(1 - \rho_n) \left(\frac{\delta}{d} \right)^{1/2} \frac{H_c B_a}{8\pi} \end{aligned} \quad (2.27)$$

We note first that if we neglect the surface terms, f_I has its minimum when $\rho_n = B_a/H_c$, or $h_n = H_c$, as expected in that case. When the surface energy is included, f_I has its minimum when

$$\rho_n = \left(\frac{B_a}{H_c} \right) \left[1 - 4 \left(\frac{\delta}{d} \right)^{1/2} \left(\frac{B_a}{H_c} \right) \right]^{-1/2} \quad (2.28)$$

At low fields this starts out as (B_a/H_c) , but the correction becomes more important at higher fields. Since we define H_{cl} as the value of B_a for which $\rho_s \rightarrow 0$ or $\rho_n \rightarrow 1$, we have, upon solving by the quadratic formula,

$$\begin{aligned} H_{cl} &= H_c \left[\left(1 + \frac{4\delta}{d} \right)^{1/2} - 2 \left(\frac{\delta}{d} \right)^{1/2} \right] \\ &\approx H_c \left[1 - 2 \left(\frac{\delta}{d} \right)^{1/2} \right] \quad d \gg \delta \end{aligned} \quad (2.29)$$

The numerical coefficient of the correction term depends on this particular detailed model, with all its approximations, but the general form of the result seems to hold for quite a variety of models.

In concluding our discussion of this very simplified model, we note that the flux density h_n in the normal regions is given by B_a/ρ_n . Using (2.28), we see that h_n decreases from H_c to H_{cl} as the applied field is increased from zero to its critical value. Thus, it is generally true that the field in the normal regions is somewhat less than H_c . Although this result may appear paradoxical, it simply reflects the role of the surface energies neglected in zeroth-order energy arguments, which consider only terms that are proportional to the volume.

REFINEMENTS. The preceding discussion of a simplified model outlines the major features of the intermediate state in a way which is certainly semiquantitatively correct in its predictions of domain size and of H_{cl} . However, it does not deal with one important qualitative feature, namely, the spreading out of the flux before it leaves the sample. This can occur most simply by having the normal domains fan out near the surface, or by more complex branching or corrugation of the domains. All these refinements increase the interface energy somewhat in order to decrease the field energy by a greater amount.

In his original treatment of the problem, Landau took into account the fanning out of the normal domains within his laminar model. The result of his numerical calculations was to replace the factor $\rho_n \rho_s h_n / H_c = \rho_s B_a / H_c$ in the denominator of (2.26) by a computed function $\phi(B_a / H_c)$ which has a qualitatively similar dependence on the applied field. Thus, this refinement has little effect on the domain size. Because of the fanning out at the surface, the flux density in the normal regions at the surface is less than the interior value, as is partially anticipated by the result of our simple model that $h_n < H_c$. It is also possible to estimate the depression of H_{cl} below H_c by considering the stability of a single isolated superconducting domain (the last one, say), taking into account the fact that the surface tension of the curved interface with the surrounding normal material effectively helps the magnetic field to destroy the last bit of superconductivity.

Curiously, Landau seems to have been somewhat unclear on the stability of this interface and he proposed a second model,⁹ in which the normal domains were assumed to branch into two, repeating as necessary, in order to spread out the flux at the surface without having the flux density in the normal regions fall below H_c . Subsequent work has shown that for samples of reasonable thickness, even a single branching would raise the free energy above that of the unbranched model because the reduction in field energy is less than the increase in interface energy. However, features resembling a Landau branching structure have been reported by Solomon and Harris¹⁰ in lead, which has a particularly low surface-energy parameter.

Extensive experimental observations by Faber¹¹ showed that a complex maze structure of corrugated normal domains was often seen. Presumably, thin normal laminae, flat in the interior, develop a corrugation of increasing amplitude as they approach the surface. This accomplishes the effective dispersal of the emerging flux over a band whose width is equal to the amplitude of the corrugation in a way which appears to be more economical of interface energy than is the branching model of Landau. Obviously, such corrugations affect the interpretation of observed domain sizes in terms of a surface-energy parameter.

It should also be mentioned that flux spots or tubes, rather than laminae, may be observed under suitable circumstances. For example, Landau pointed out that normal tubes should be more favorable at low flux density, whereas superconducting tubes should be more favorable for the last superconducting material near H_c . Experiments¹² of Träuble and Essmann have revealed a regular array of flux spots in lead foils in a perpendicular field, whereas Kirchner¹³ has observed both flux spots and laminalike "meanders" in rather similar samples. The

⁹L. D. Landau, *Nature* **141**, 688 (1938); *J. Phys. U.S.S.R.* **7**, 99 (1943).

¹⁰P. R. Solomon and R. E. Harris, *Phys. Rev.* **B3**, 2969 (1971).

¹¹T. E. Faber, *Proc. Roy. Soc. (London)* **A248**, 460 (1958).

¹²H. Träuble and U. Essmann, *Phys. Stat. Sol.* **25**, 395 (1968).

¹³H. Kirchner, *Phys. Lett.* **26A**, 651 (1968).

evolution of the flux pattern with increasing field from flux tubes to corrugations, then branches, and finally into superconducting tubes at high fields is particularly clearly demonstrated by motion pictures taken by various groups¹⁴ using the magneto-optic technique. Evidently, the richness of the phenomena observed in the intermediate state poses a severe challenge to any complete theoretical understanding. Yet another dimension of complexity is added in the time-dependent phenomena of the dynamic intermediate state, but we shall not go into that aspect here.

2.3.3 Intermediate State of a Sphere

To illustrate the application of our results in a more general geometry, we now return to the case of the sphere. As found previously, the intermediate state will exist when $\frac{2}{3} < H_a/H_c < 1$. In this range, the volume of the sphere is subdivided into S and N laminae, which fan out near the surface and may branch or become corrugated, but we shall ignore these refinements in the present discussion. Moreover, we shall assume that the radius of the sphere is large enough compared to the domain-wall thickness δ so that we can ignore the difference between H_{cl} and H_c . Then the flux density in the N laminae is always exactly H_c , and the normal fraction ρ_n is B/H_c , where \mathbf{B} is the average of $\mathbf{h}(\mathbf{r})$ over the laminar structure. In the macroscopic Maxwell equations, this average serves for \mathbf{B} everywhere inside the sphere. On the other hand, the magnitude of the Maxwell \mathbf{H} in the sphere throughout the intermediate state is just H_c . This follows since $H = h = H_c$ in the normal laminae, and the tangential component of \mathbf{H} is continuous across the interface between laminae since the only currents there are internal ones associated with the medium in thermodynamic equilibrium. Thus, as is the case in more familiar examples, the macroscopic fields inside the sphere are uniform, whereas those outside are the sum of the applied field plus a dipole field, namely,

$$\mathbf{B} = \mathbf{H} = \mathbf{H}_a + \frac{H_1 R^3}{2} \nabla \left(\frac{\cos \theta}{r^2} \right) \quad (2.30)$$

This has the same form as the expression (2.18) which we found to hold in the linear regime before $2H_c/3$; in that case, the parameter H_1 was chosen to equal H_a , so as to match $B_n = 0$ at $r = R$. In the intermediate state, $B_n \neq 0$. Rather, we determine H_1 by equating the internal and external values of B_n and of H_{tang} :

$$B_n = B \cos \theta = H_a \cos \theta - H_1 \cos \theta \quad (2.31)$$

¹⁴See, e.g., P. R. Solomon and R. E. Harris, *Proc. 12th Int'l. Conf. on Low Temp. Phys.*, Kyoto, Japan (1970), p. 475.

$$H_{\text{tang}} = H_c \sin \theta = H_a \sin \theta + \frac{1}{2} H_1 \sin \theta \quad (2.32)$$

Solving, we find $H_1 = \frac{2(H_c - B)}{3}$, so that

$$B = 3H_a - 2H_c \quad \frac{2}{3} \leq \frac{H_a}{H_c} \leq 1 \quad (2.33)$$

Thus, the magnetic induction of the sphere increases linearly from zero to H_c as the applied field H_a increases from $2H_c/3$ to H_c , as depicted in Fig. 2.3.

Because B_n is continuous, B can be measured external to the sphere by measuring B at the pole, $\theta = 0$. Similarly, the continuity of H_{tang} implies that the internal value of H can be measured externally by measuring the equatorial surface field, $B_{\text{equat}} = H_{\text{equat}}$. The predicted dependence of this quantity is also shown in Fig. 2.3. Experimental data on clean samples actually follow these predictions quite well.

2.4 INTERMEDIATE STATE ABOVE CRITICAL CURRENT OF A SUPERCONDUCTING WIRE

As our final example of dc electrodynamics of type I superconductors, we now discuss the appearance of resistance in a superconducting wire above its critical current. Consider a wire of radius a carrying a current I . By Maxwell's equation, the magnetic field at the surface of the wire is $2I/ca$. When this equals H_c , the wire can no longer be entirely superconducting. As noted in Sec. 2.2.2, this defines a critical current

$$I_c = \frac{H_c ca}{2} \quad (2.34)$$

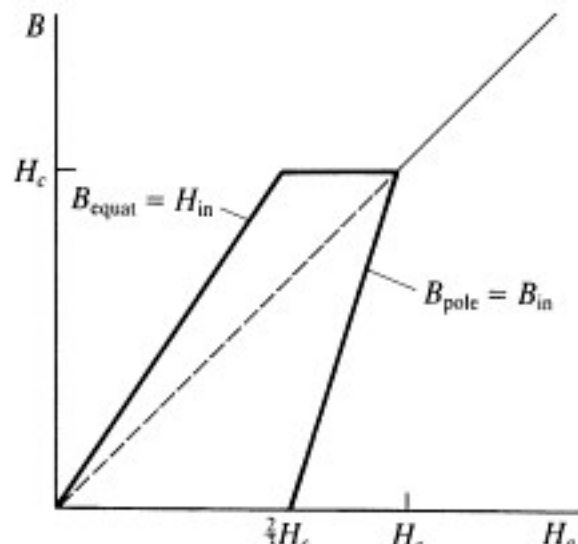


FIGURE 2.3

Internal values of B and H in a superconducting sphere in an applied field H_a . As indicated, these can be measured externally by measuring the surface field B at the pole and the equator, respectively. The sphere is in the intermediate state for $2H_c/3 < H_a < H_c$.

based on Silsbee's rule that the critical current cannot exceed that which produces a critical magnetic field at the superconductor. (The critical current may be much less than is given by this criterion, especially if the thickness of the superconductor is much less than λ .) If $I > I_c$, then the surface field exceeds H_c , and the surface (at least) must become normal.

But if a surface layer were to go normal and to leave a fully superconducting core, the current would all go through the core, leading to a still greater field at its surface, which would a fortiori be greater than H_c . Thus, no stable configuration exists with a solid superconducting core surrounded by normal material. What if the sample went entirely normal? In this case, the current density J would be uniform across the cross section, leading to

$$H(r) = \frac{2Ir}{ca^2}$$

Since this drops below H_c as $r \rightarrow 0$, the core could not be wholly normal either.

These observations suggest a core region (of radius $r_1 < a$) in an intermediate state, surrounded by a normal layer which also carries current. The latter requires a longitudinal electric field, which is compatible with an intermediate-state structure, so long as its layers are oriented transverse to the axis.

The nature of the intermediate-state structure is dictated by the requirement that, neglecting surface energies, $H(r) = H_c$ for $r \leq r_1$. Since $H(r) = 2I(r)/cr$, where $I(r)$ is the total current inside radius r , we need $I(r) = crH_c/2$. This requires a current density

$$J(r) = \frac{1}{2\pi r} \frac{dI}{dr} = \frac{cH_c}{4\pi r} \quad (2.35)$$

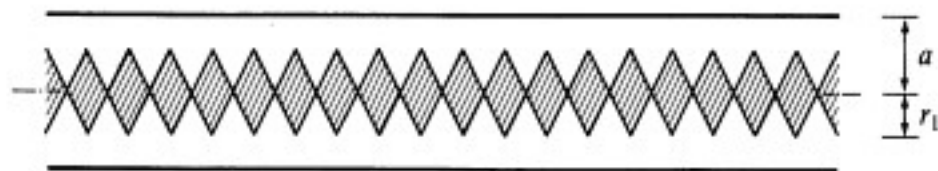
Yet, the longitudinal electric field E is independent of r , as can be seen since $\text{curl } \mathbf{E} = -(1/c)(\partial \mathbf{B}/\partial t) = 0$ if we assume the structure is stable in time. These requirements are approximately reconciled by the configuration shown in Fig. 2.4, first proposed by F. London,¹⁵ in which the fractional path length (parallel to the axis of the wire) of resistive material is r/r_1 . If the normal resistivity is ρ , this leads to

$$J(r) = \frac{Er_1}{\rho r}$$

for $r < r_1$. Combining this with (2.35), we see that

$$r_1 = \frac{\rho c H_c}{4\pi E} \quad (2.36)$$

¹⁵F. London, "Une Conception Nouvelle de la Supraconductibilité," *Act. Sci. et Ind.*, no. 458, Hermann & Cie., Paris (1937). A more accessible discussion may be found on p. 120 in London's book *Superfluids*, vol. I, Wiley, New York (1950).

**FIGURE 2.4**

London's model of the intermediate-state structure in a wire carrying a current in excess of I_c . The shaded region is superconducting. The core radius r_1 is a at I_c and ideally approaches zero only asymptotically as $I \rightarrow \infty$.

Since the current inside the core I_1 must generate a field H_c at the surface of the core, we have

$$I_1 = \frac{cr_1 H_c}{2} = \frac{c^2 H_c^2 \rho}{8\pi E}$$

The current in the outer normal layer is

$$I_2 = \frac{E}{\rho} \pi (a^2 - r_1^2) = \frac{\pi a^2 E}{\rho} - \frac{c^2 H_c^2 \rho}{16\pi E}$$

Adding this to I_1 , we obtain the total current in the wire

$$I = \frac{\pi a^2 E}{\rho} + \frac{c^2 H_c^2 \rho}{16\pi E} \quad (2.37)$$

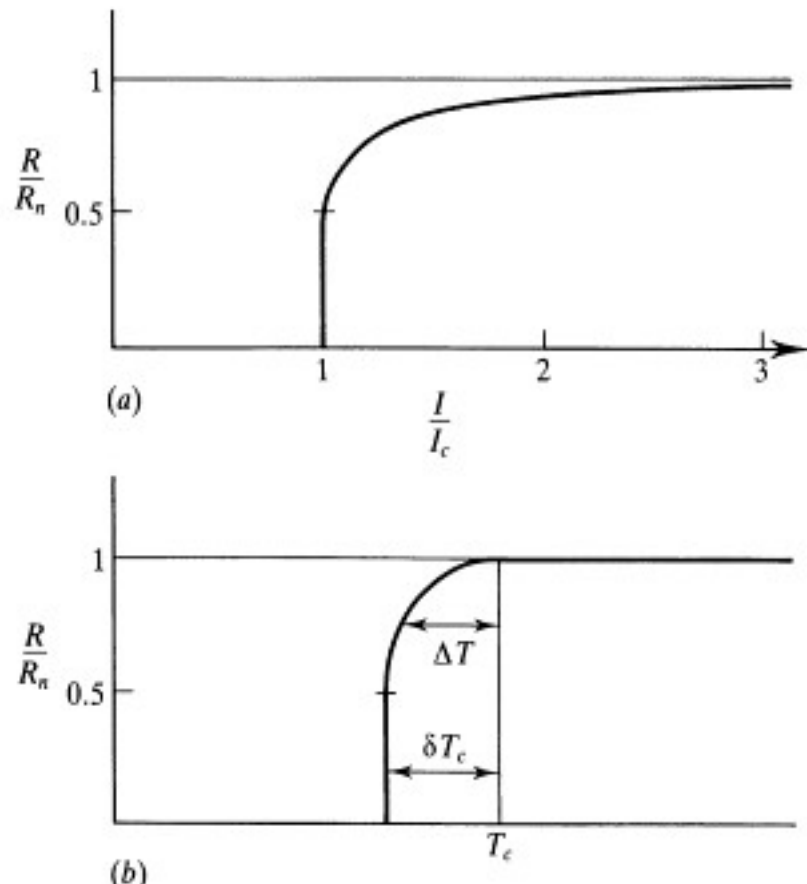
Solving the quadratic equation for $E(I)$, and using (2.34), we find

$$E = \frac{\rho I}{2\pi a^2} \left\{ 1 \pm \left[1 - \left(\frac{I_c}{I} \right)^2 \right]^{1/2} \right\} \quad (2.38)$$

The plus sign must be chosen if E is to increase with an increase of I , as required for stability. Note also that in the normal state $E = \rho I / \pi a^2$, by the usual Ohm's law relation. Thus, we can write our results in terms of an apparent fractional resistance

$$\frac{R}{R_n} = \begin{cases} 0 & I < I_c \\ \frac{1}{2} \left\{ 1 + \left[1 - \left(\frac{I_c}{I} \right)^2 \right]^{1/2} \right\} & I > I_c \end{cases} \quad (2.39)$$

From this we see that half the resistance appears discontinuously at I_c , at which point the intermediate-state pattern suddenly fills the entire wire. With further increase of current, the resistance increases continuously as the intermediate-state region shrinks to a smaller and smaller central core, the asymptotic behavior being $r_1/a = I_c/2I$. In principle, some superconducting material will continue to exist in the core for all finite currents. In practice, however, the Joule heating above I_c makes it hard to carry out an isothermal experiment to confirm this property in detail.

**FIGURE 2.5**

Resistance of a wire in the intermediate state. (a) Current dependence at constant temperature. (b) Temperature dependence at constant current, showing the broadening and depression of the apparent transition temperature. The parameter $\delta T_c = I(dI_c/dT)^{-1}$.

Experimental data are in good qualitative agreement with the theoretical result (2.39), which is plotted in Fig. 2.5, but there are quantitative discrepancies. In particular, the discontinuous jump in resistance typically goes from zero to 0.7–0.8 R_n , rather than to $\frac{1}{2}R_n$, as predicted by the simple theory.¹⁶ This has led to a number of reexaminations of the London model. For example, Gorter¹⁷ considered a dynamic model, with continually moving phase boundaries. On the other hand, Baird and Mukherjee¹⁶ have made more detailed numerical studies of static models similar to London's. They were able to find the optimum ratio of domain period to wire diameter (~ 0.7), and the curved domain-wall profiles on which $H = H_c$ and which come closer than the London model to truly satisfying the condition that $H = H_c$ throughout (rather than doing so only on the average

¹⁶D. C. Baird and B. K. Mukherjee, *Phys. Lett.* **25A**, 137 (1967), and references cited therein. See also B. K. Mukherjee, J. F. Allen, and D. C. Baird, *Proc. 11th Intl. Conf. on Low Temp. Phys.*, St. Andrews (1968), p. 827.

¹⁷C. J. Gorter, *Physica* **23**, 45 (1957).

over the domain structure). In this improved static model, they did find a larger jump in R/R_n (to 0.69) at I_c , and generally improved agreement at higher currents as well. A third approach, by Andreyev and Sharvin,¹⁸ combines these ideas to consider a broad class of moving structures. This approach also leads to a larger jump in R/R_n at I_c of about the correct size even though apparently depending on different parameters from the static theory mentioned earlier. Thus, although the theoretical position is still somewhat unclear, there is no doubt that the London theory of the intermediate state in a current-carrying wire is oversimplified. Nonetheless, it provides a useful semiquantitative treatment of the problem.

This theory can also be applied to predict the temperature dependence of the resistance of a superconducting wire as it goes through its transition near T_c . In this temperature region, $I_c \propto H_c \propto (T_c - T)$, so we can write

$$I_c = \frac{dI_c}{dT} \Big|_{T_c} \Delta T \approx c a H_c(0) \frac{\Delta T}{T_c}$$

With the London approximation (2.39), this leads to

$$\frac{R}{R_n} = \frac{1}{2} \left\{ 1 + \left[1 - \left(\frac{\Delta T}{\delta T_c} \right)^2 \right]^{1/2} \right\} \quad (2.40)$$

where $\Delta T = T_c - T$, and $\delta T_c = I(dI_c/dT)^{-1}$. For example, if a measuring current of 1 A (ampere) were used in a 1-mm diameter tin wire, the first onset of resistance would occur about 0.03 K below T_c . Thus, in a critical-temperature measurement, I must be kept small enough so that the δT_c from this source is negligible compared to the intrinsic breadth of the transition as limited by sample inhomogeneity. The shape of the resistive transition due to finite current is illustrated in Fig. 2.5b.

There is also a current-induced intermediate state in thin-film superconductors. Although the geometry is much less simple to handle theoretically because of edge effects, this configuration has the advantage that the intermediate-state structure can be viewed by a magneto-optic technique. Experiments by Huebener and collaborators¹⁹ have shown that the resistance increases in discrete increments, each associated with the appearance of an additional channel for the motion of magnetic-flux tubes across the strip. The fact that the flux pattern is moving can be demonstrated by the observation of an induced voltage in another adjacent superconducting film in a thin-film sandwich. In these experiments, a time of flight of the order of 10^{-3} sec could be inferred from noise-spectrum measurements. In other experiments, such as those of L. Rinderer, and those of

¹⁸A. F. Andreyev and Yu. V. Sharvin, *Zh. Eksperim. i Teor. Fiz.* **53**, 1499 (1967); see also A. F. Andreyev, *Proc. 11th Int'l. Conf. on Low Temp. Phys.*, St. Andrews (1968), p. 831.

¹⁹R. P. Huebener and R. T. Kampwirth, *Solid State Comm.* **10**, 1289 (1972); R. P. Huebener and D. E. Gallus, *Phys. Rev. B7*, 4089 (1973).

Solomon and Harris cited earlier, motion pictures have been taken of the moving domain patterns under situations in which the motion is much slower. These experimental results confirm that some sort of time-dependent structure is characteristic of resistive regimes in superconductors. We shall return to this point in connection with dissipative effects in type II superconductors in Chap. 5.

2.5 HIGH-FREQUENCY ELECTRODYNAMICS

In the *static* examples treated in earlier sections of this chapter, the superconductor has been described entirely in terms of a lossless diamagnetic response, except for the completely normal domains created in response to strong fields and currents. Most practical applications of superconductivity, however, involve ac currents, whether at low frequencies in power lines or at high frequencies in microwave and computer applications, and superconductors always show finite dissipation when carrying alternating currents. The reason for this is simple. According to the first London equation, a *time-varying* supercurrent requires an electric field \mathbf{E} to accelerate and decelerate the superconducting electrons. This electric field also acts on the so-called "normal" electrons (really thermal excitations from the superconducting ground state, as we shall see in Chap. 3), which scatter from impurities, and can be described by Ohm's law. In this section, we introduce the so-called *two-fluid model*, which describes the electrodynamics that results from the superposition of the response of the "superconducting" and "normal" electron fluids to alternating electromagnetic fields. Although this model is, of course, an oversimplification, it is the standard working approximation for understanding electrical losses in superconductors, so that dissipation can be anticipated and minimized in applications such as microwave resonators. The validity of the model is restricted, however, to frequencies below the energy-gap frequency, since above that frequency additional loss mechanisms set in and the dissipation approaches that in the normal state.

2.5.1 Complex Conductivity in Two-Fluid Approximation

In the Drude model, introduced in Sec. 2.1, the drift velocity of the electron gas, as governed by Newton's second law, obeys the equation

$$m \frac{d\mathbf{v}}{dt} = e\mathbf{E} - m\mathbf{v}/\tau \quad (2.41)$$

In a general two-fluid model, one assumes that the total electron density n can be divided into two parts: the density of superconducting electrons is n_s and that of normal electrons is n_n , and they have different relaxation times τ_s and τ_n in (2.41). If one crudely models the behavior of the superconducting electrons simply by assuming $\tau_s = \infty$, as we did in motivating the first London equation, the last term drops out, and we obtain the first London equation (1.3) in the form $d\mathbf{J}_s/dt = (n_s e^2/m)\mathbf{E} = (c^2/4\pi\lambda^2)\mathbf{E}$. The normal electrons give a parallel ohmic

conduction channel, with $\mathbf{J}_n = (n_n e^2 \tau_n / m) \mathbf{E}$, provided that $\omega \ll 1/\tau_n$ (as is typically the case even at microwave frequencies).

So long as we are interested only in the *linear* response of the superconductor, it is very convenient to Fourier analyze the applied electric field and to treat the response to each frequency separately. According to (2.41), the ac response of either parallel channel ($i = n, s$) to a field $Ee^{i\omega t}$ is described by a complex conductivity

$$\sigma_i(\omega) \equiv \sigma_{1i}(\omega) - i\sigma_{2i}(\omega) = (n_i e^2 \tau_i / m) / (1 + i\omega\tau_i) \quad (2.42)$$

whose real and imaginary parts are

$$\sigma_{1i}(\omega) = \sigma_{0i} / (1 + \omega^2 \tau_i^2) \quad (2.43a)$$

$$\sigma_{2i}(\omega) = \sigma_{0i} \omega \tau_i / (1 + \omega^2 \tau_i^2) \quad (2.43b)$$

where $\sigma_{0i} \equiv n_i e^2 \tau_i / m$. If we now describe the superconducting electrons by letting τ_s increase continuously to ∞ , we see that the $\sigma_{1s}(\omega)$ curve becomes higher and higher at $\omega = 0$ but cuts off at a lower and lower frequency, retaining a constant area under the curve. Eventually, it shrinks to a δ function $\sigma_{1s}(\omega) = (\pi/2)(n_s e^2 / m)\delta(\omega)$, the strength of which can be confirmed by an elementary integration of $\int \sigma_{1s}(\omega) d\omega$ over positive frequencies. In this same limiting process, $\sigma_{2s}(\omega)$ approaches the limit $n_s e^2 / m\omega$, which is equivalent to the first London equation. For both the normal and superconducting components, the area under the $\sigma_{1i}(\omega)$ curve has the value $(\pi/2)n_i e^2 / m$, proportional to n_i and independent of τ_i , as required by the general quantum mechanical *oscillator strength sum rule*, although we have used a classical model. In the historical Gorter-Casimir two-fluid model, it was thought that $n_n \sim t^4$ and $n_s \sim (1-t^4)$, where $t = T/T_c$. Such a dependence is consistent with the often used empirical approximation that $\lambda \sim (1-t^4)^{-1/2}$. The modern picture, described in a later chapter, is more complicated, but the temperature dependences are qualitatively similar.

Since this treatment applies only to frequencies below the energy gap, it is usually possible to assume that frequencies are also low enough so that $\omega\tau_n \ll 1$. In that case, the combined response of the two fluids to an electric field reduces simply to

$$\sigma_1(\omega) = (\pi n_s e^2 / 2m)\delta(\omega) + n_n e^2 \tau_n / m \quad (2.44a)$$

$$\sigma_2(\omega) = n_s e^2 / m\omega \quad (2.44b)$$

This approximation is qualitatively very useful, despite its obvious limitations. The essential importance of the normal fluid contribution is that it provides *nonzero* dissipation in superconductors *at all nonzero frequencies*. For example, this accounts for the finite Q in superconducting microwave cavities, as we shall see in detail subsequently.

2.5.2 High-Frequency Dissipation in Superconductors

The ideal dc properties of superconductors are governed by the flow of lossless supercurrent within an equilibrium state of the system. We now examine the response of a superconductor to a high-frequency current, in which the normal electrons give a finite amount of dissipation because the supercurrent response is no longer a zero-impedance shunt. To proceed, we use the approximate two-fluid expressions (2.44) for the complex conductivity. From these expressions we see that at any nonzero frequency, the conductivity has a real part $\sigma_1 = n_n e^2 \tau_n / m$ and an imaginary part $\sigma_2 = n_n e^2 / m\omega$, where n_n and n_s are the densities of normal and superconducting electrons, respectively, in this model description.

It may be helpful to use a circuit analogy, in which σ_1 is the conductance $1/R$ of a resistive channel in parallel with an inductive channel of admittance $1/i\omega L$. This circuit has a characteristic frequency, $\omega_0 = R/L$, below which the dominant current flow is in the lossless inductive channel and above which the resistive channel dominates. Returning to the superconducting case, the ratio of currents in the two channels is

$$\frac{J_s}{J_n} = \frac{n_s e^2 / m\omega}{n_n e^2 \tau_n / m} = \frac{n_s}{n_n \omega \tau_n} \quad (2.45)$$

Thus, the crossover frequency will be $\omega \approx (n_s/n_n)(1/\tau_n)$.²⁰ Since τ_n is typically $\sim 10^{-12}$ sec, the crossover frequency will be typically $\sim 10^{11}$ Hz (Hertz) if n_s/n_n is of order unity. In the historic two-fluid approximation, the temperature dependence of this ratio is given by $n_s/n_n \approx (1 - t^4)/t^4$. In a more modern version based on the energy gap Δ in the BCS theory, $n_n \sim e^{-\Delta/kT}$, which has the same qualitative behavior as t^4 but goes to zero exponentially at low temperatures instead of as a power law. We conclude that at frequencies below the high-microwave range, most of the current will be carried as a supercurrent, but there will be *nonzero* dissipation from the normal component for any nonzero frequency, even one that is orders of magnitude below the crossover frequency.

To make this argument more quantitative, we start by noting that realistic experimental arrangements usually involve a *current bias* as opposed to a *voltage bias* because superconductors have much lower impedance than typical sources of electrical energy, causing the external source to be the current-limiting element in the circuit. Given an imposed ac current density J , the power dissipated per unit volume is $\rho J^2 = \text{Re}(1/\sigma)J^2 = [\sigma_1/(\sigma_1^2 + \sigma_2^2)]J^2 \approx (\sigma_1/\sigma_2^2)J^2$, where in the last step we have used the fact that typically $\sigma_1 \ll \sigma_2$. Despite its simplicity, this argument is generally sound and leads to two important and correct conclusions. First, the

²⁰Actually, in a BCS superconductor with $\omega_g \tau \ll 1$, a better approximation to the crossover frequency is $n\omega_g/n_n$. Here $\omega_g = \Delta/\hbar$ is the energy-gap frequency. This does not change the order of magnitude estimate of the crossover frequency.

frequency dependence of the dissipation is $\sim \omega^2$ because of the factor $1/\sigma_2^2$. Physically, this reflects the fact that the dissipation is $\sigma_1 E^2$, and that the electric field E required to accelerate a given amplitude supercurrent must rise as ω because the acceleration of the electrons must be accomplished in a shorter time period $\sim 1/\omega$. The second important conclusion is that the dissipation is proportional to σ_1 , i.e., the density of normal electrons, since they provide the mechanism by which the electric field dissipates energy. [It should be remembered that these conclusions only hold for frequencies with photon energies that are lower than the BCS energy gap, which is $\sim kT_c$. Above that frequency ($\sim 10^{11} - 10^{12}$ Hz), there is little difference between the superconducting and normal-state dissipation properties.]

As a concrete example, we consider the surface resistance and absorptivity of a superconducting surface such as those forming the walls of a microwave cavity. For simplicity, we consider the response to an incoming plane wave at normal incidence. Because the metal impedance is so low compared to free space, the incident wave is almost perfectly reflected, forming a standing wave with a maximum of H at the surface. The amplitude of the oscillating H at the surface is twice the incident amplitude H_{inc} because of the constructive superposition of incident and reflected waves at the surface. Applying the Maxwell equation $\text{curl } \mathbf{H} = 4\pi\mathbf{J}/c$, the discontinuity between $h = 2H_{\text{inc}}$ outside the surface and $h = 0$ inside implies a surface *sheet* current density $\mathcal{J} = cH_{\text{inc}}/2\pi$ flowing in the skin layer of depth δ . (This is an example of the *current bias* mentioned in the preceding paragraph.) The dissipated power per unit area is then $\mathcal{J}^2 R_s$, where R_s is the *surface resistance*, i.e., the resistance per square of the surface layer of thickness δ . By solving the skin-depth problem for a general complex conductivity, we find $\delta = c[2\pi\omega(|\sigma| + \sigma_2)]^{-1/2}$, and then

$$R_s = \delta^{-1} \operatorname{Re}(1/\sigma) = \delta^{-1} \sigma_1 / |\sigma|^2 \approx \delta^{-1} \sigma_1 / \sigma_2^2 \quad (2.46)$$

The physical significance of this surface resistance is made more evident by using it to compute the absorptivity \mathcal{A} of the surface, i.e., the fraction of the incident electromagnetic energy which is absorbed. Using the magnitude of the Poynting vector to obtain the incoming power, we obtain the following:

$$\mathcal{A} = \frac{P_{\text{abs}}}{P_{\text{inc}}} = \frac{\mathcal{J}^2 R_s}{c H_{\text{inc}}^2 / 4\pi} = \frac{c}{\pi} R_s \quad (2.47)$$

Thus, the surface resistance is a direct measure of the absorptivity of the surface.

Applying (2.47) to the normal state of a metal, where $\sigma_1 = \sigma_n$ and $\sigma_2 = 0$, we find the familiar result

$$\mathcal{A}_n = (2\omega/\pi\sigma_n)^{1/2} \quad (2.47a)$$

In the superconducting state, the corresponding result is

$$\mathcal{A}_s \approx (2\sigma_1\omega^{1/2})/(\sigma_2^{3/2}\pi^{1/2}) \propto \omega^2\sigma_1 \quad (2.47b)$$

in agreement with our general result for the dependence on frequency and σ_1 . The different frequency dependences of (2.47a,b) are of practical importance. Since the normal absorptivity rises only as $\omega^{1/2}$ whereas the superconducting absorptivity rises as ω^2 , the difference between them narrows as the frequency increases, even well below the energy-gap frequency, above which \mathcal{A}_s rapidly rises to equal \mathcal{A}_n .

Since these absorptivities are typically less than 10^{-3} and can be as small as 10^{-10} in superconductors, they are difficult to measure in a single reflection. However, in a resonant microwave cavity with superconducting walls, the radiation is reflected many times as it bounces around in the cavity, thus magnifying the absorption. Experimentally, the level of dissipation in a resonator is described by its Q or *quality factor*, which is defined as the energy stored divided by the energy dissipated per radian (i.e., a time interval of $1/\omega$). This Q also describes the width Δf of the resonant response of the cavity since it can be shown that $\Delta f/f = 1/Q$.

We can approximately relate Q to \mathcal{A} by the steps indicated in the following equation:

$$Q = \frac{\text{stored energy}}{\text{loss per radian}} = \frac{(H^2/8\pi)V}{(c/4\pi\omega)H^2\mathcal{A}S} = \frac{\omega V}{2c S \mathcal{A}} \approx \frac{L}{\lambda} \frac{1}{\mathcal{A}} \approx \frac{1}{\mathcal{A}} \quad (2.48)$$

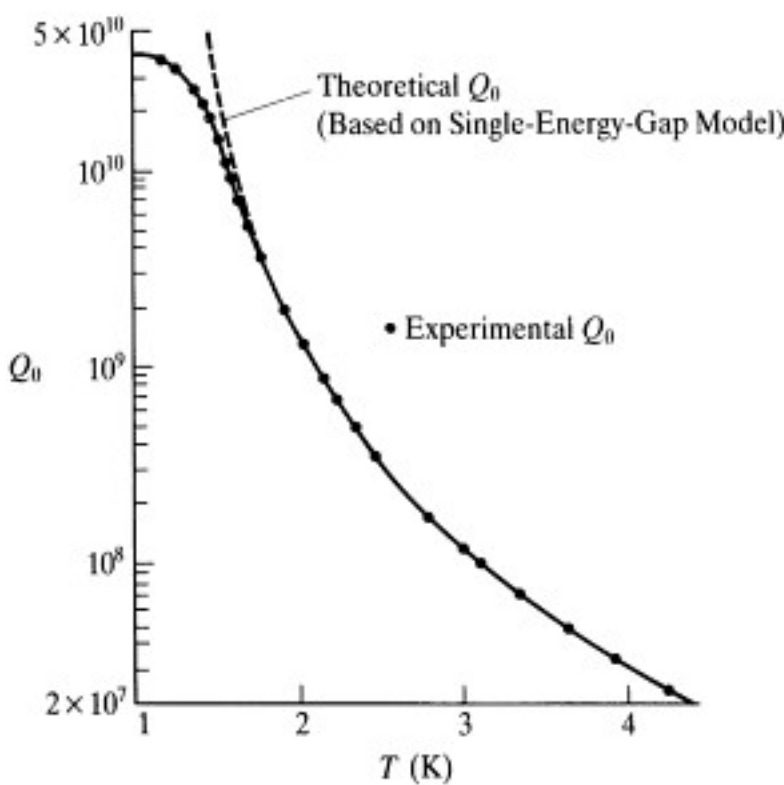


FIGURE 2.6

Temperature dependence of Q_0 for a 11.2-GHz niobium cavity. [After Turneaure and Weissman, J. Appl. Phys. 39, 4417 (1968).]

In (2.48), V is the volume of the cavity, S is its surface area, $L = V/S$ is a typical linear dimension of the cavity, and λ is the wavelength of the radiation. The last step is appropriate only if the cavity is operating in its lowest mode, so that its linear dimension is of the order of the wavelength; at best, (2.48) is only roughly valid. Despite the crude approximations, (2.48) provides a useful guide to understanding the relation between absorptivity and cavity Q . With superconducting cavities, Q values as high as 10^{10} have been achieved, indicating extremely low absorption compared to normal metals, for which typically $Q \leq 10^4$. The temperature dependence of the Q of a niobium cavity is shown in Fig 2.6. The exponentially rapid variation reflects the freezing out of normal electrons, causing $n_n(T)$ to fall approximately as $e^{-\Delta/kT}$, where Δ is the BCS energy gap. Such high- Q cavities are of technical importance in applications as very narrow-band microwave filters. For example, a Q of 10^{10} implies a frequency resolution of 1 Hz in a cavity resonant at 10^{10} Hz.